Bill Johns email: "*the workshop needs to include more discussion of issues related to the atmospheric circulation in the tropical Atlantic, including especially the PBL and related impacts on surface fluxes and their accuracy.*"

Chris Fairall, NOAA/ESRL
Paquita Zuidema U of Miami

Responses:

- accuracy of flux products
- recent US CLIVAR WG on Eastern Tropical Ocean Biases findings
- recent atmospheric field campaigns
- regions of particular interest (equatorial Atlantic, upwelling regions)

Surface flux measurements from buoys, ships, and gridded products; Atmospheric and marine boundary layer observations

Christopher W. Fairall
NOAA ESRL/PSD
Boulder, CO

1. Background
2. Observing
3. Ship and buoy intercomparisons
4. COARE bulk flux algorithm
5. Gridded flux products

OVERVIEW - PSD air-sea flux program

- Fits with Tropical buoy array, ORS buoys, SAMOS, gridded flux products. Advances science of air-sea interaction and observing technology
- State-of-the-art ship-based direct flux measurements
  - Momentum, energy, water, trace gas surface budgets
  - Side-by-side with ships, buoys, satellites, NWP, flux products
  - Flux database for science, parameterization, community comparisons
- Maintain and advance COARE family flux algorithms
  - Meteorological, gas transfer, air-sea-ice, hurricanes

PSD1 Measurements: Hardware

Goal: State-of-the-art accuracy

- Wind speed: 3-D sonic anemometer
  - Motion corrected, flow distortion corrected
- Air T, RH, P: Vaisala system
  - Ventilated radiation shield
- SST: PSD sea snake
  - Floating thermistor
- Radiative flux: Eppley/Kipp-Zonen radiometers
  - Calibrated at GMD Boulder
- Rain rate: Long path optical scintillometer
  - No wind speed-induced error
- Fast Humidity/CO2: IR absorption
- Trace Gases: Partner

PSD Roving Ship Calibration Standard for Air-Sea Fluxes: Example STRATUS 2017

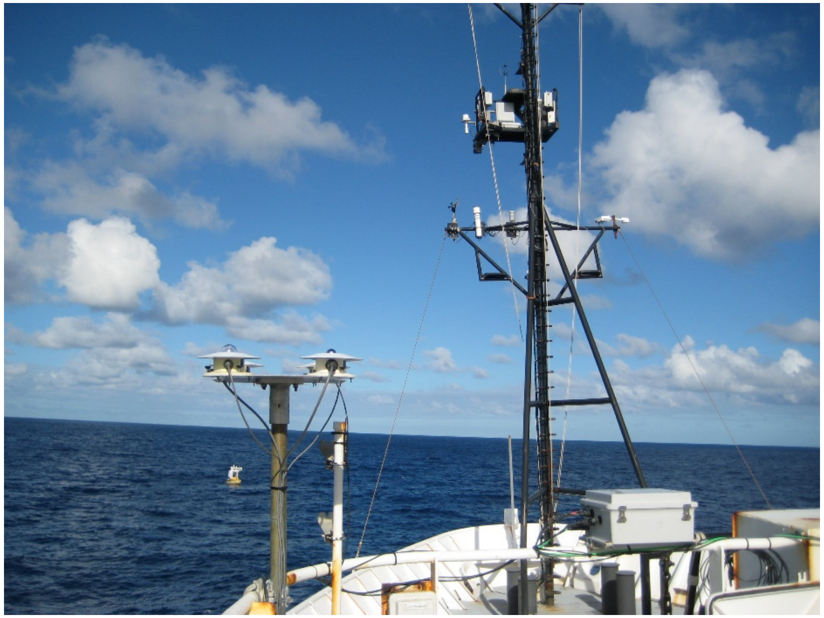

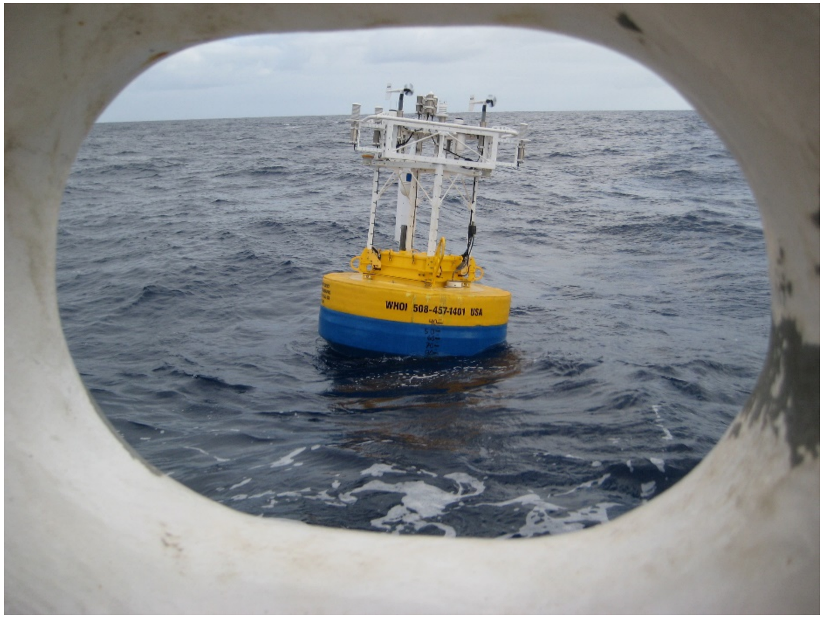

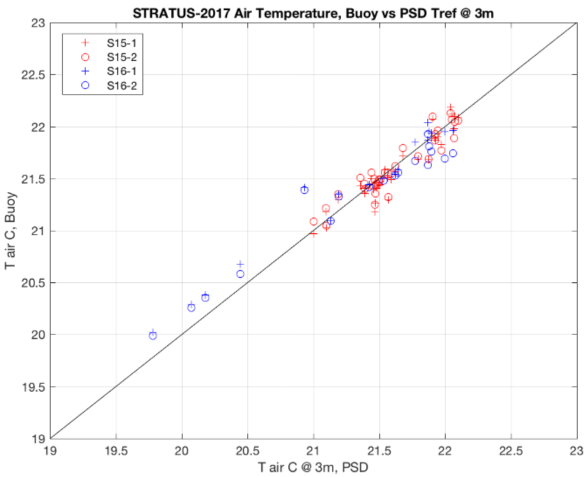

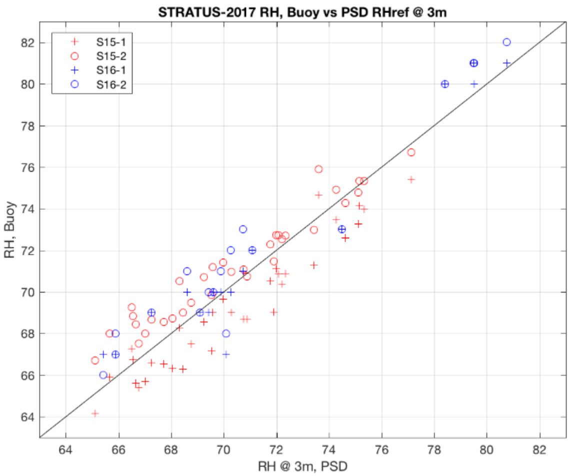

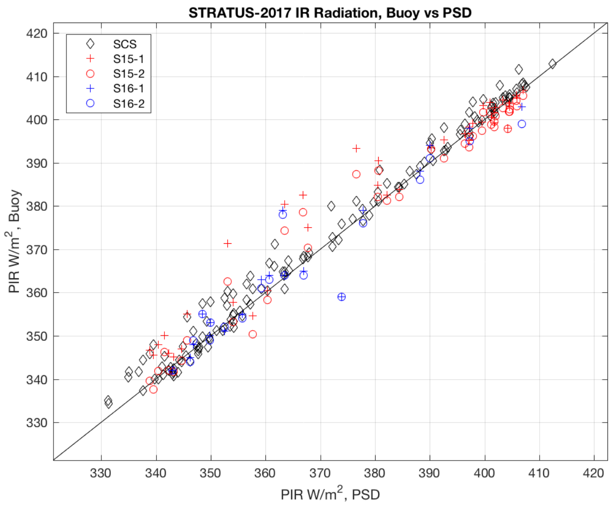

Evaluation of Flux Reference Buoy Accuracy: 10 Years of Data

Table 1. Comparison of PSD ship and WHOI buoy observations from 10 years of observations at the Straus buoy (20 S 85 W) for the period 2000-2010.								
Variable	Buoy	Ship	Δ_1	σ_1	$\Delta_{0.25}$	$\sigma_{0.25}$	$\sigma_{1/N}^{1/2}$	SAMOS
SST, C	18.90	19.01	0.11	0.18	0.12	0.16	0.006	0.1
U, m/s	6.49	6.63	0.14	0.96	-0.05	0.61	0.03	0.2
T_{air}, C	18.20	18.26	0.07	0.35	0.10	0.32	0.01	0.2
Qair, g/kg	9.65	9.58	-0.08	0.42	-0.19	0.36	0.01	0.3
RH, %	74.6	74.7	-0.9	3.9	-1.9	2.7	0.12	2
P, mb	1018.3	1017.3	-1.0	2	-0.5	1.8	0.07	2
SWR, W/m^2	223.7	223.9	0.3	83	-6	78	2.7	5
LWR, W/m^2	377.4	381.0	3.5	14.5	4.9	12.9	0.5	5
H_s, W/m^2	-5.9	-6.3	-0.4	5.0	0	3.7	0.16	5
H_l, W/m^2	-93.0	-101.0	-7.0	14.3	-7.7	14.3	0.55	5
τ, N/m^2	0.080	0.080	0.0	0.023	-0.005	0.016	5e-4	-
H_N, W/m^2	78	75	-2.9	73	-7.7	67	2.4	10

Comparison of the ship and buoy platforms for all cases (N=939) when the ship was within 1 degree of the nominal buoy position and for 510 cases when the ship was within 0.25 degrees. The PSD mean wind, air temperature, and humidity were computed from PSD heights (zu_psd=17.7 m; zt_psd=15.5 m) to the same height as the buoy sensors (zu_buoy 3.3 m; zt_buoy=2.89 m) using the reference feature in the algorithm. From these results we can examine the mean bias (Δ) and 1-hrly standard deviation (σ), which will depend on the horizontal separation limits (we chose 1 degree and 0.25 degree.

Synthesis of Research Vessel Meteorological Measurement Accuracy

Ship	Ts C	Ta C	Qa g/kg	RH %	U m/s	Rl W/m^2	Rs W/m^2	P mb
RHB 99 - 03	-0.1	-0.1	**-0.7**		0.2			
KAI 00 - 02	0	0.2	0.4		0.4			
Revelle 03	0.2	-0.2	0		**0.8**		4	
RHB 04	-0.1	-0.1	-0.1		-0.2	-1	2	
Tao Buoys 99-04	-0.05	0.2	0.5		0.3	1	**-12**	
Knorr 08		-0.2	-0.2	-0.5	-0.3	0	5	1
RHB 08	-0.3	0.3	**1.3**	**7**	-0.2	0	6	-0.1
Kilo Moana 09	0.3	**-0.8**	**-0.7**	-1	0.4	2	**-11**	
RHB 10	-0.3	0	0.4	3	**-0.7**	3	**-16**	-0.1
Atlantis 10	0.1	0.4	0.4	-1	**-0.7**		**-25**	
Hi'Illikai 11	**-0.4**	**1.7**	**0.9**	2	0.4			-0.8
Revelle 11	-0.1	0.2	0.1	0	0.1	3	8	0.3
Mean	-0.07	0.13	0.19	1.36	0.04	1.14	-4.33	0.06
Sigma	0.2	0.6	0.6	2.9	0.5	1.6	11.8	0.7
Sigma/sqrt(N-1)	0.06	0.17	0.17	1.03	0.13	0.56	3.74	0.27
SAMOS target	**0.1**	**0.1**	**0.15**	**1**	**0.2**	**3**	**3**	**0.5**
PSD Standard	**0.1**	**0.2**	**0.3**	**2**	**0.2**	**5**	**5**	**0.3**

- Analysis of 10 years of comparisons of the PSD roving flux standard with NOAA and UNOLS research vessel meteorological observations reveals inconsistent accuracy for some vessels.
- The analysis shows the R/V fleet taken as an ensemble has no significant bias in variables used to compute fluxes, although individual ships have accuracy problems
- SST, IR flux, and pressure are generally within guidelines. The yellow highlighting indicates variables where ships are still not adequate.

The PSD Air-Sea Flux Database Version 2.0

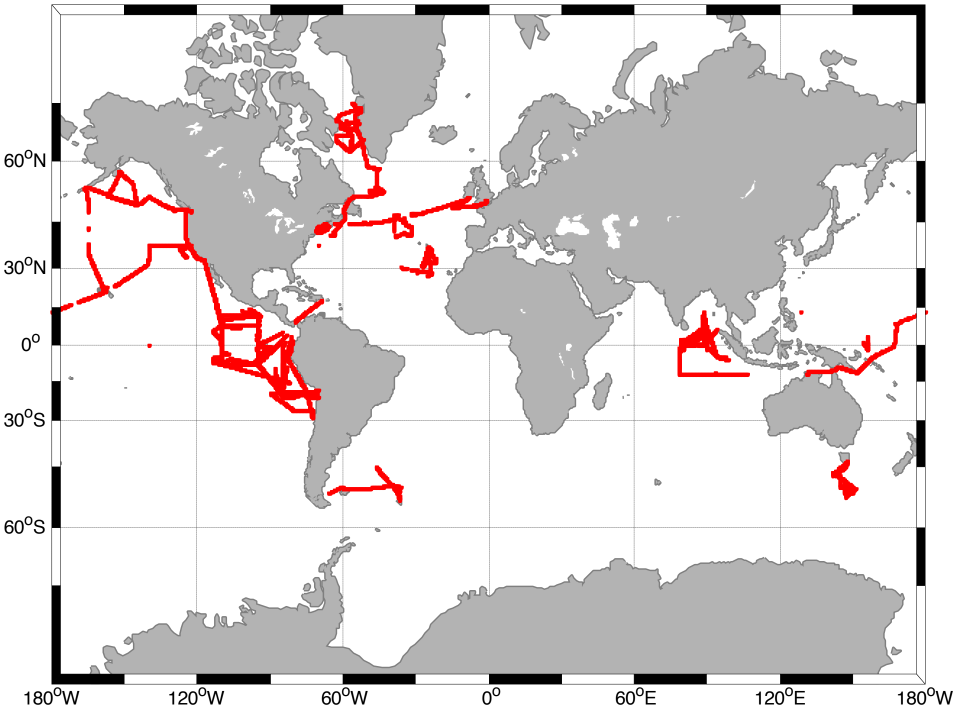

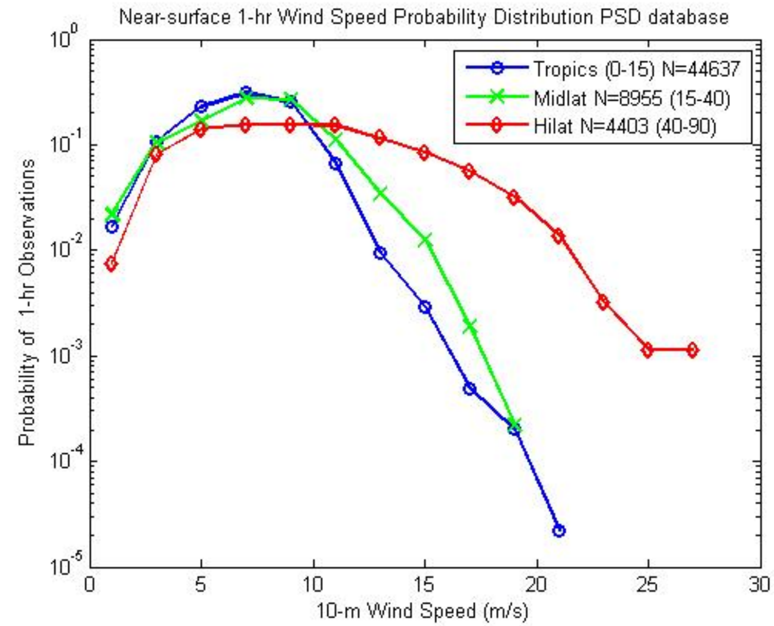

Some preliminary results for the new PSD flux data base combining observations from 30 cruises (a total of 25,000 1-hr observations). Map of cruise tracks (upper left), wind speed probability distributions in three latitude bands (upper right). Surprisingly the tropics and subtropics have similar PDF's; the high latitude distributions is broader and has a higher mean wind speed. Grand comparison of direct covariance and inertial dissipation (ID) vs the NOAA COARE bulk algorithm surface stress (momentum flux) estimates (lower right).

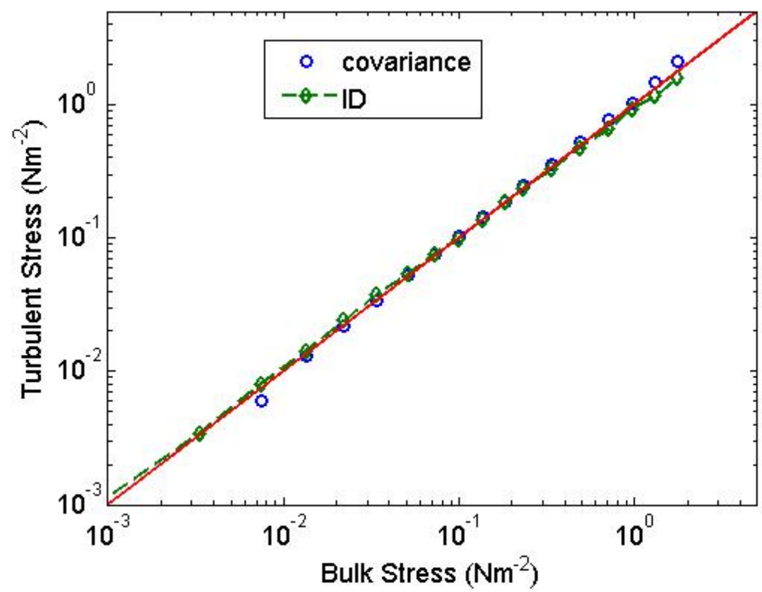

Summary Evaluation of In Situ Errors

		For daily averages			Contribution to			
	Flux	**er**	**Std**	**Std/er**	**er(TAU)**	**er(Q0)**	**er(E-P)**	**er(FCO2)**
Variable					Nt/m^2	W/m^2	mm/day	$mol/m^2/yr$
wind speed (m/s)	all	0.1	1.75	17.5	0.0027	2.1	0.053	0.12
SST (C)	all	0.1	1.45	14.5	0.0002	4.4	0.081	0.0083
air temp. (C)	all	0.1	1.30	13.0	0.0002	3.6	0.075	0.0089
rel. hum. (percent)	all	2.7	4.83	1.8	0.0002	11.9	0.32	0.012
SWR (W/m^2)	Q0	6	42.00	7.0	0	5.6	0	0
LWR (W/m^2)	Q0	4	13.75	3.4	0	3	0	0.0012
sfc currents (m/s)	all	0.05	0.25	5.0	0.0008	0.65	0.017	0.04
BP (hPa)	FCO2	0.2	1.48	7.4	0	0	0	0.0002
Rain (mm/day)	E-P	0.72	5.34	7.4	0	0	0.7	0
air pCO_2 (μatm)	FCO2	3	0.00	0.0	0	0	0	0.12
wat pCO_2 (μatm)	FCO2	4	0.00	0.0	0	0	0	0.086
Total of meas. errors					**0.0027**	**14.3**	**0.81**	**0.19**
Meas. error for covariance fluxes					0.0008	8.2	0.7	0.10
Total meas. and sampling error for cov. fluxes					**0.0021**	**9.2**	**0.7**	**0.15**
					TAU	**Q0**	**E, P, E-P**	**FCO2**
Mean (across equator)					0.039	125.6	2.0,1.9,0.12	3.2

Table 1 from WP

Present Status of *Surface* Flux Parameterizations
Tuned to Direct Observations

Turbulent Fluxes: Bulk Parameterization

Mean correlation of turbulent variables represented in terms of mean flow variables – wind speed, surface-to-air variable difference

MetFlux – Dominated by atmospheric turbulent xfer

GasFlux – Dominated by oceanic molecular xfer; Enhanced by whitecap bubbles

$$Met\ Flux: \overline{w'x'} = C_x U (X_s - X_r) = C_x U \Delta X$$

$$Gas\ Flux: \overline{w'x'} = k_x \alpha_x \Delta X \qquad \alpha = sol.$$

$$Particles: F_{source} = F(f_{whitecap}, U, u_*, wave\, breaking, slope)$$

HIWINGS 2015

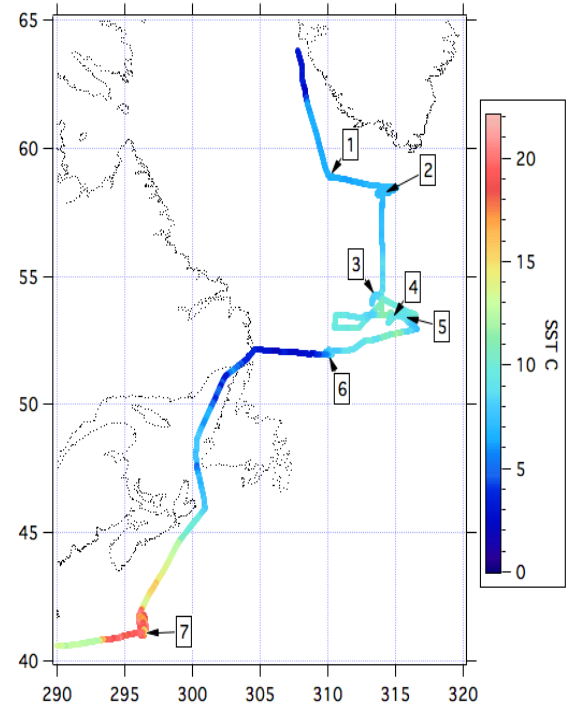

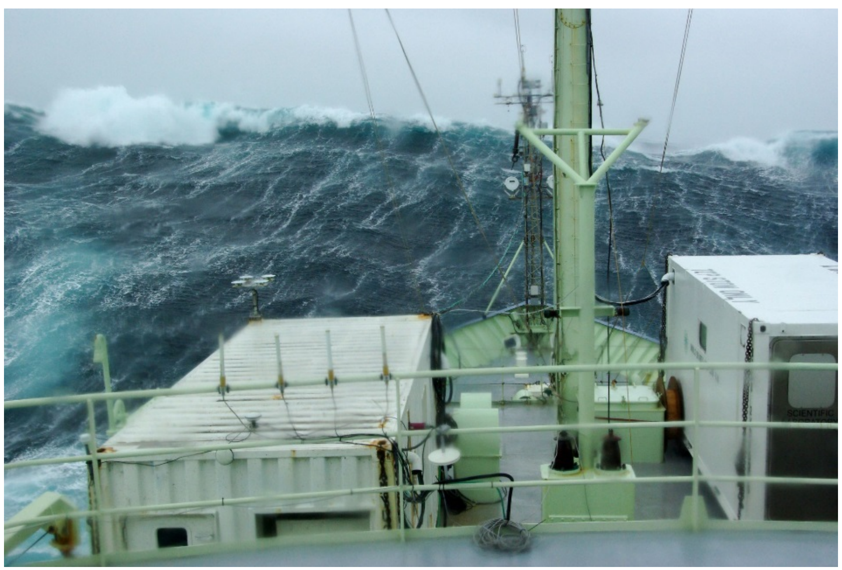

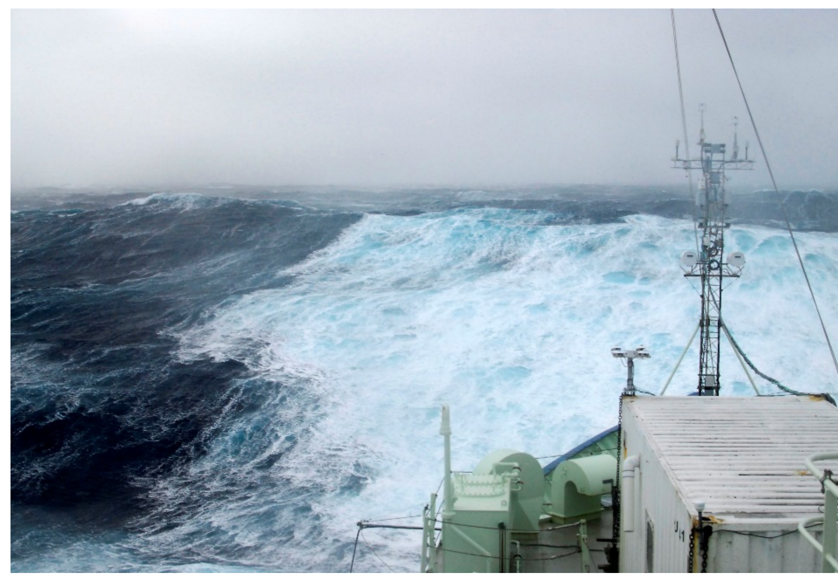

COARE Algorithm

Table 2. History of the COARE bulk algorithms.		
Year	Version and Function	Collaborators
1996	2.5 Met fluxes, cool skin, diurnal warm layer	UConn, CSIRO
2000	CO2	UConn, LDEO, WHOI
2003	3.0 Met fluxes	UConn, CSIRO
2004	DMS	UHawaii
2005	Snow and Ice	CRREL
2006	Ozone	UColo INSTAR
2008	PCB and PCE	Mich. Tech. U.
2011	3.1G Gas fluxes: CO2, CO, O3, DMS, He, SF6	UConn, LDEO, UHawaii, UColo INSTAR
2013	3.5 Met fluxes	UConn, WHOI, SUNY, OSU
2018	3.6 Met, 3.6G Gas, 3.5I Ice-air-water fluxes	UConn, UNSW, LDEO

Algorithms and updates: 11 pubs 4500 citations

Progress on Flux Measurements: Historical vs HIWINGS

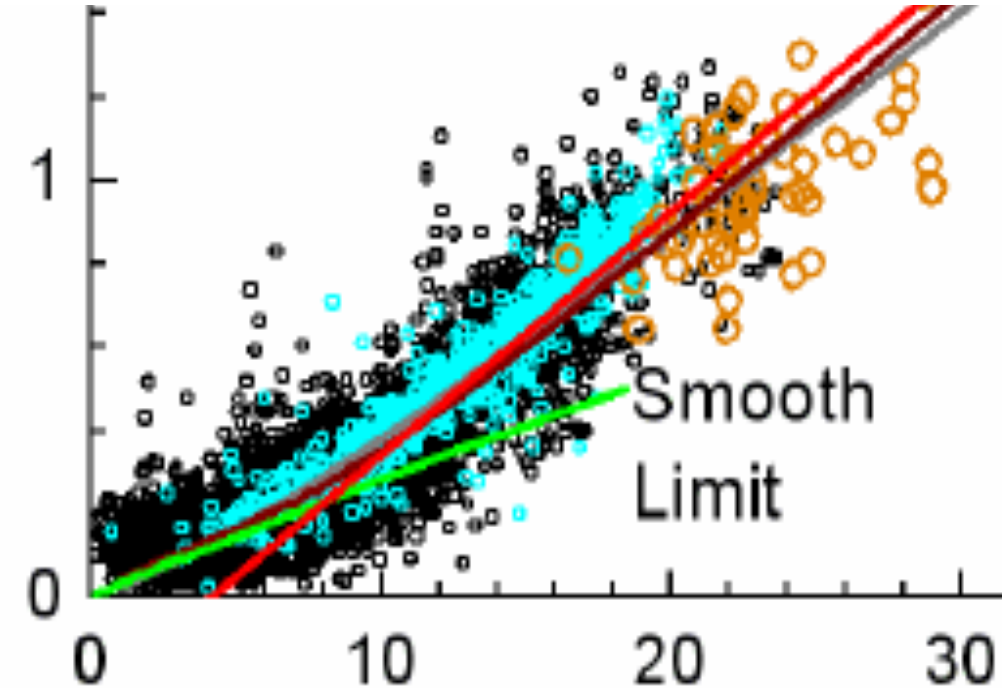

Cyan – Ship database
Black – Mahrt Aircraft database
Orange – CBLAST aircraft

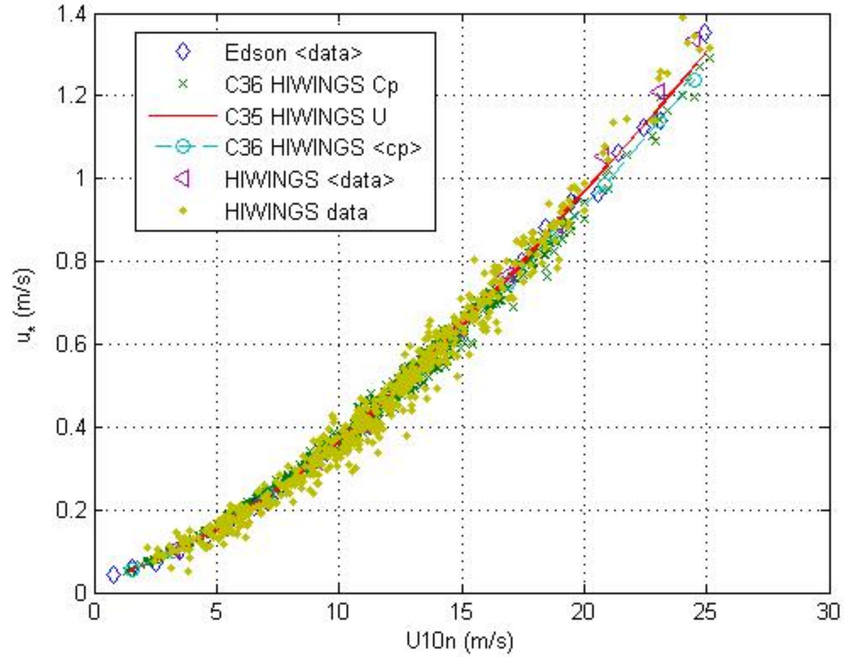

PSD Observations from HIWINGS
Big symbols – averages in windspeed bins
Red line – C35 Cd(U)
X's – Cd(U, Cp, Hs)
Green dots – One hr u_* observations

Community Flux Products:

- NWP: SURFA Archived flux fields from ECMWF, DWD, JMA

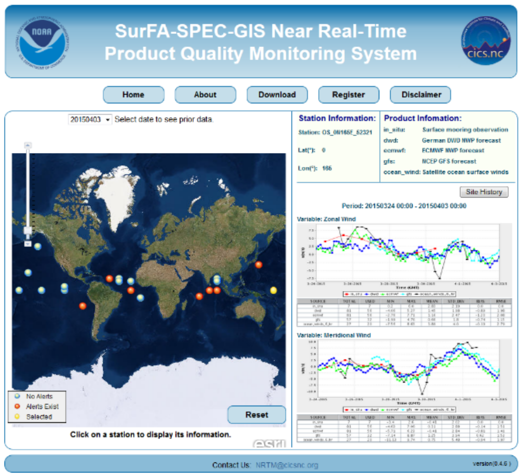

- Blended: WHOI OAFlux, CORE,..

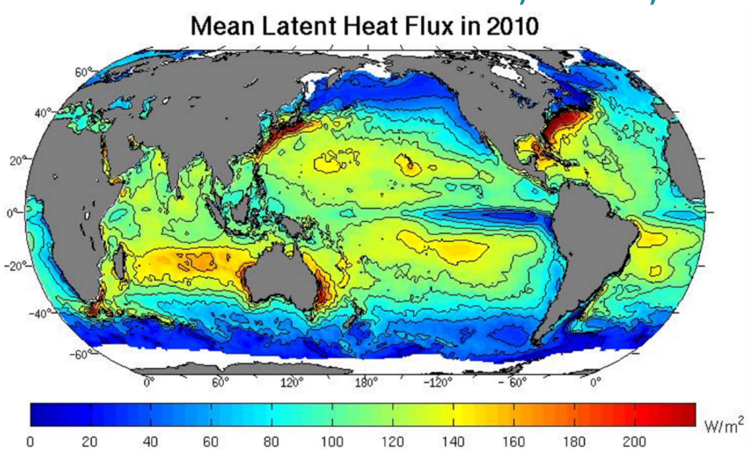

Satellite: SEAFLUX, GSSTF, HOAPS, JOFURO, IFREMER

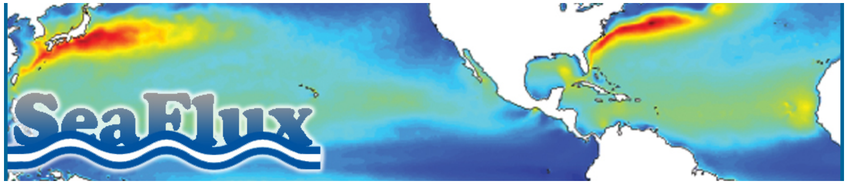

Most flux products estimate fluxes with bulk relationships. They obtain gridded values for wind speed, humidity, SST, air temperature, then compute flux estimates:

$$Met\ Flux : \overline{w'x'} = C_x S(X_s - X_r) = C_x S \Delta X$$

$$H_{latent} = \rho L_e \overline{w'q'}$$

Accuracy for 10 W/m^2 net guideline

wind speed	2% or 0.2 m/s
SST, Ta	0.1 C
RH	2%

Mean Qnet

of 11 products

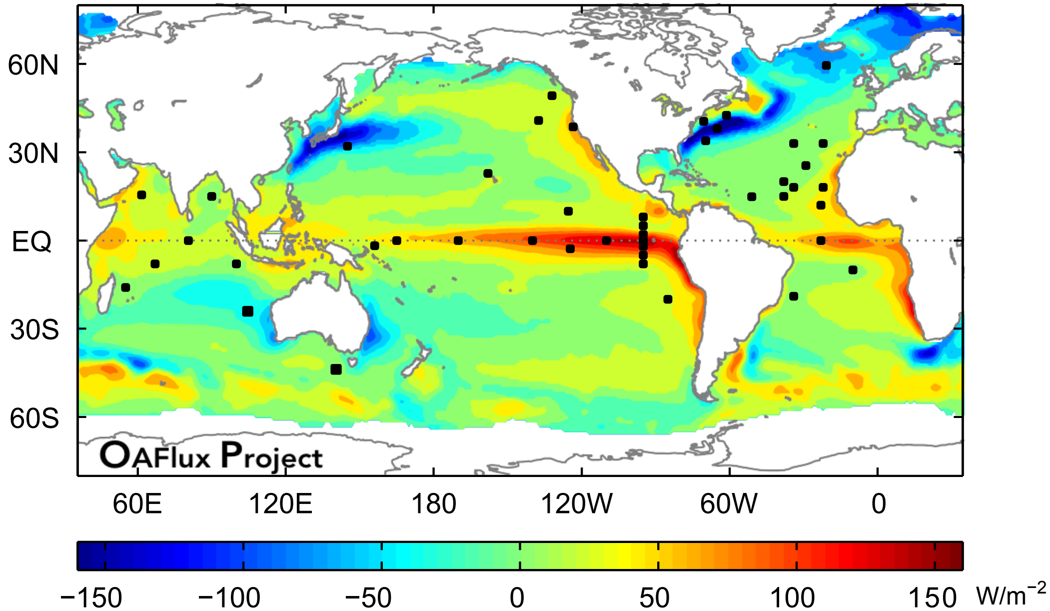

Courtesy L. Yu
And M. Cronin

STD Qnet

of 11 products

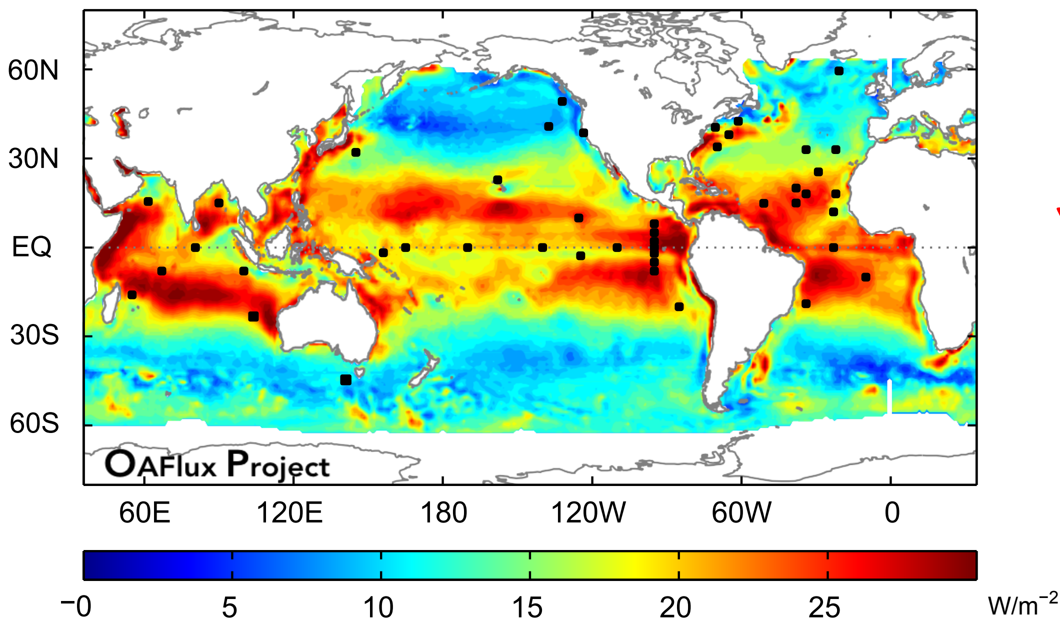

Yikes!

Products: OAFlux, NOC2, ERAinterim, MERRA, CFSR, ERA40, NCEP1, NCEP2, CORE2, ISCCP, NASA/SRB, CERES

Tropical Comparisons

DYNAMO:
Equatorial Indian Ocean 2011

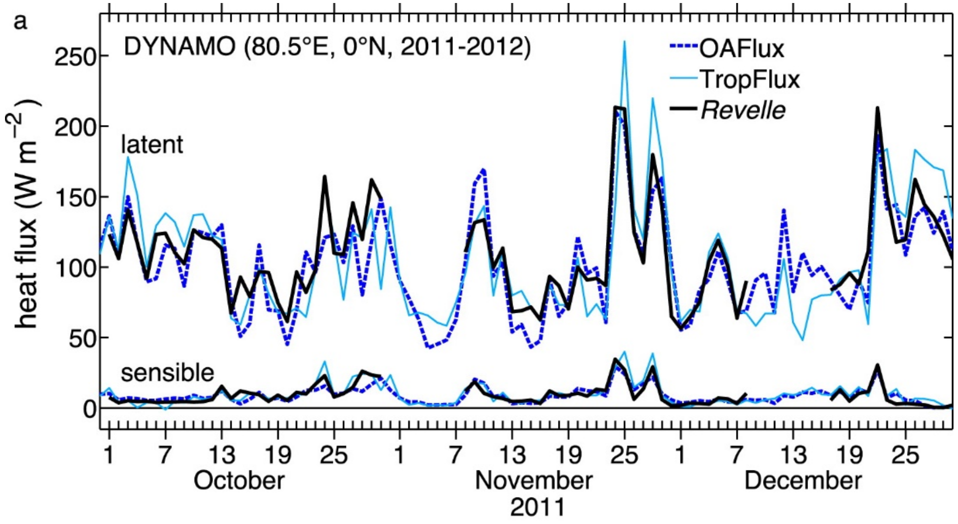

TOGA COARE:
Equatorial W. Pacific Ocean
1992-1993

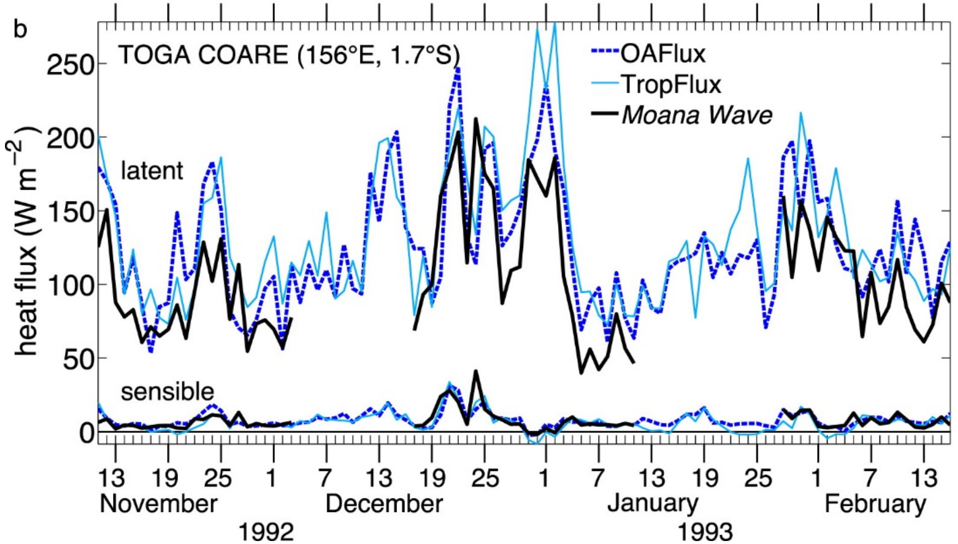

East Pacific Equatorial Cruises

ESRL-PSD Tao Buoy Maintenance Cruises, 6 October and 3 April deployments: flux, boundary-layer, cloud systems

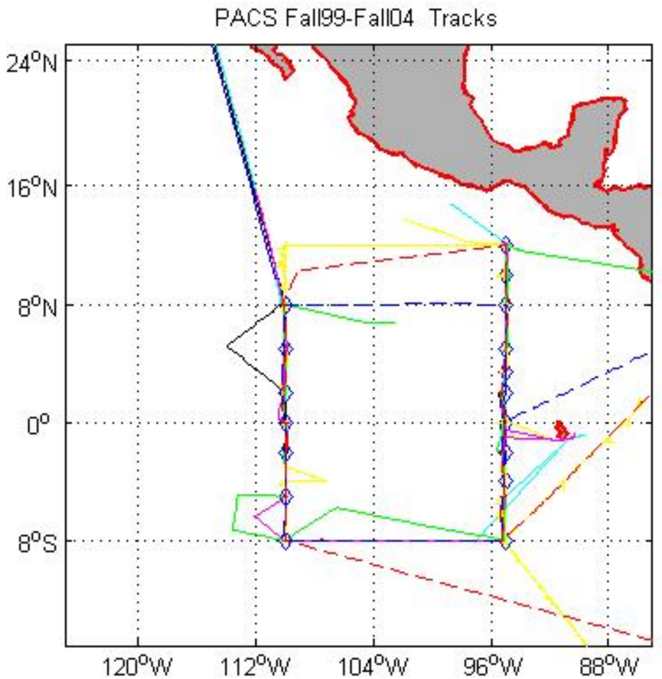

GFDL Coupled Model - IPCC

U. Hawaii Regional

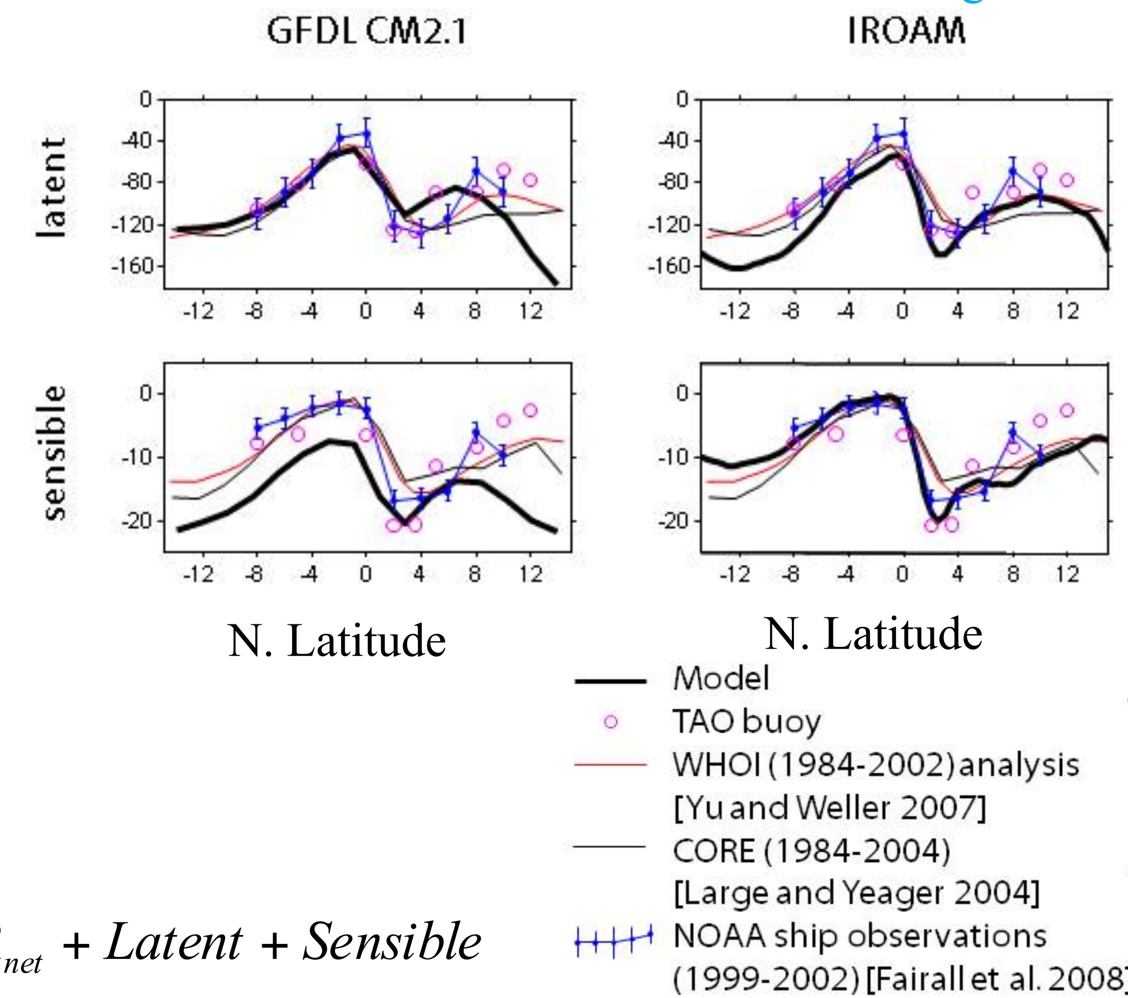

$$NetHeatFlux = Solar_{net} + IR_{net} + Latent + Sensible$$

		For daily averages			Contribution to			
	Flux	**er**	**Std**	**Std/er**	**er(TAU)**	**er(Q0)**	**er(E-P)**	**er(FCO2)**
Variable					Nt/m^2	W/m^2	mm/day	$mol/m^2/yr$
wind speed (m/s)	all	0.1	1.75	17.5	0.0027	2.1	0.053	0.12
SST (C)	all	0.1	1.45	14.5	0.0002	4.4	0.081	0.0083
air temp. (C)	all	0.1	1.30	13.0	0.0002	3.6	0.075	0.0089
rel. hum. (percent)	all	2.7	4.83	1.8	0.0002	11.9	0.32	0.012
SWR (W/m^2)	Q0	6	42.00	7.0	0	5.6	0	0
LWR (W/m^2)	Q0	4	13.75	3.4	0	3	0	0.0012
sfc currents (m/s)	all	0.05	0.25	5.0	0.0008	0.65	0.017	0.04
BP (hPa)	FCO2	0.2	1.48	7.4	0	0	0	0.0002
Rain (mm/day)	E-P	0.72	5.34	7.4	0	0	0.7	0
air pCO_2 (µatm)	FCO2	3	0.00	0.0	0	0	0	0.12
wat pCO_2 (µatm)	FCO2	4	0.00	0.0	0	0	0	0.086
Total of meas. errors					**0.0027**	**14.3**	**0.81**	**0.19**
Meas. error for covariance fluxes					0.0008	8.2	0.7	0.10
Total meas. and sampling error for cov. fluxes					**0.0021**	**9.2**	**0.7**	**0.15**
					TAU	**Q0**	**E, P, E-P**	**FCO2**
Mean (across equator)					0.039	125.6	2.0,1.9,0.12	3.2

Table 1 from WP

Atlantic Tradewind Ocean-Atmosphere Mesoscale Interaction Campaign – ATOMIC
A study of shallow convection and ocean coupling in the N Atlantic

- EUREC4A - a field campaign to elucidate the couplings between clouds, convection and circulation
  - European effort of Barbados winter 2020
  - Aircraft, ships, Island-based systems
  - Extensive regional LES modeling effort
  - Emphasis on the role of shallow convection in climate model CO2 warming sensitivity
- US involvement (ATOMIC)
  - Leverage EUREC4A effort
  - Take advantage of unique capabilities of NOAA observing assets
  - Take advantage of historical collaboration of Universities and Fed Labs
  - Emphasis on shallow convection, mesoscale coupling with the ocean, aerosol-cloud

Shallow Convection Looking Down

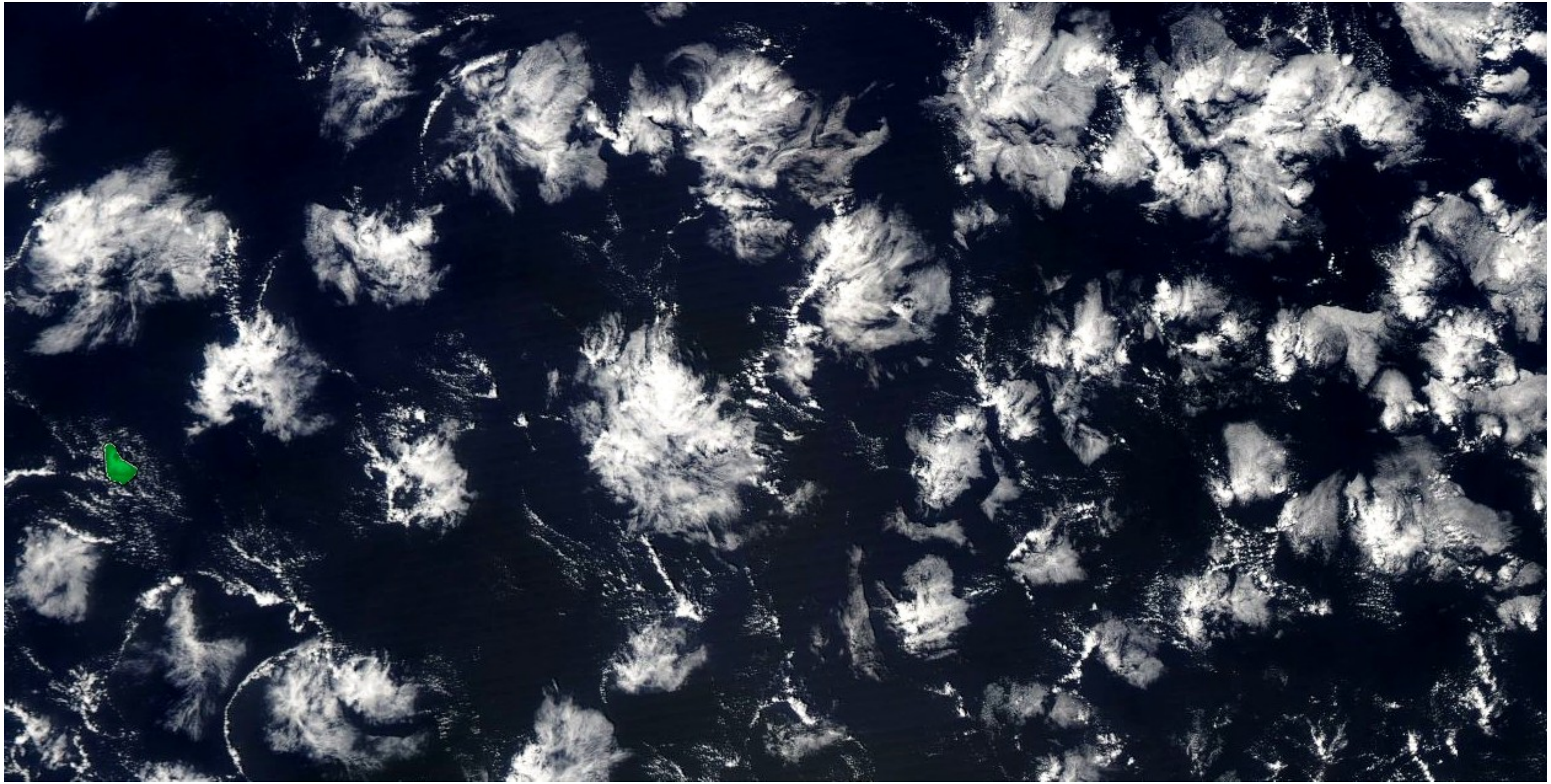

Radar Looking Up

Shallow

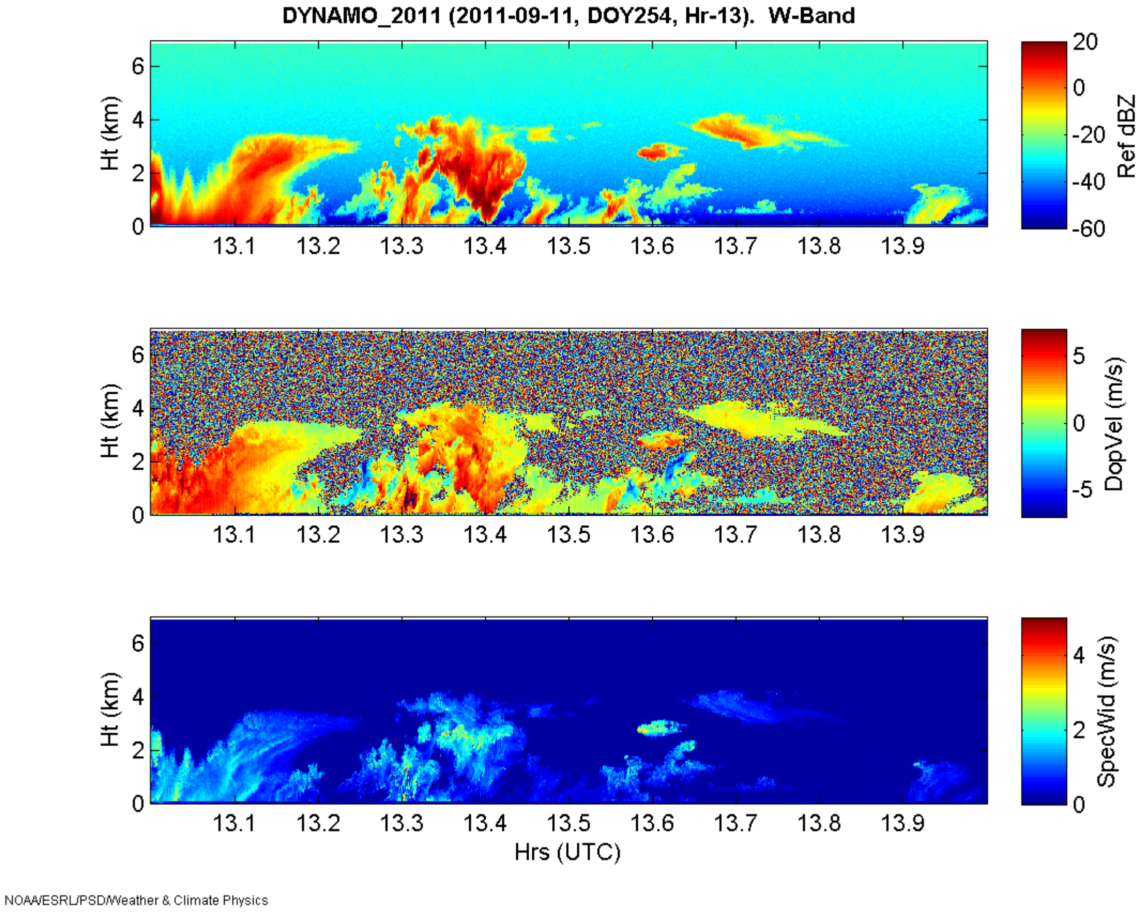

Deep

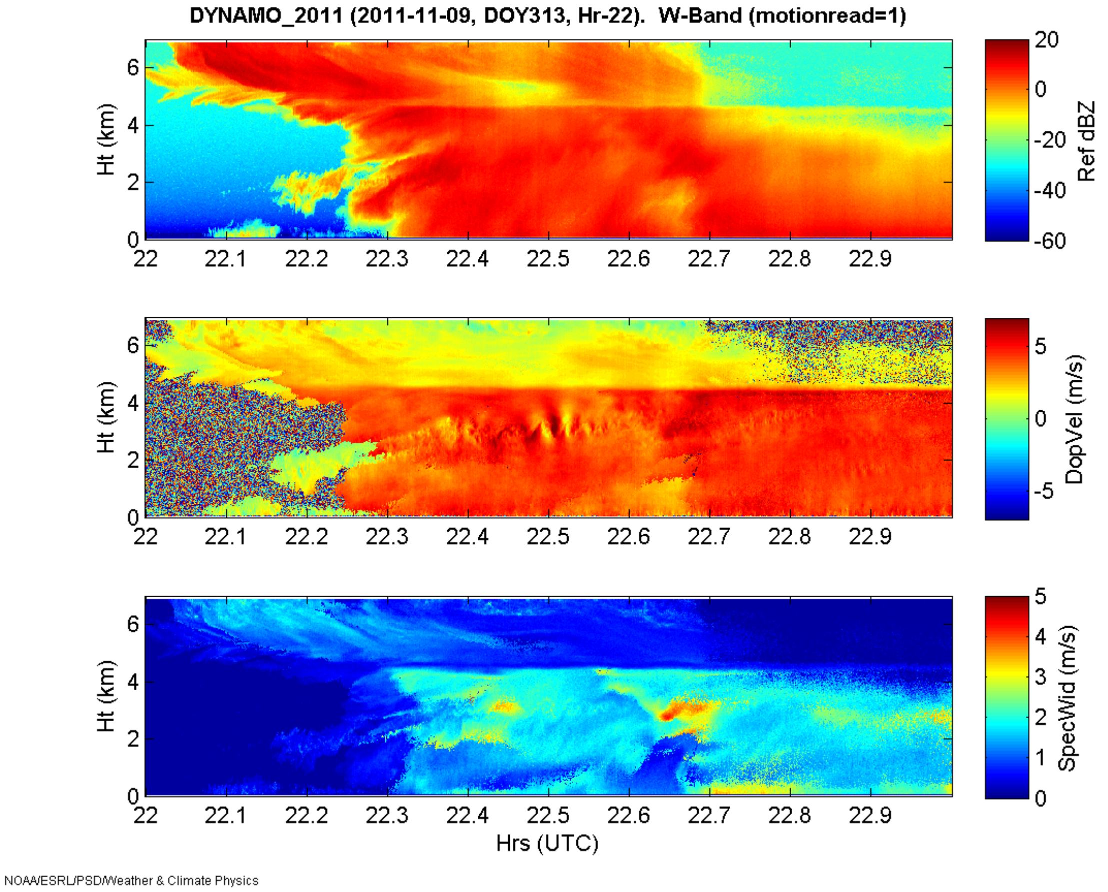

Science Points

- Shallow convection influences:
  - Climate sensitivity
  - MJO propagation
  - Hurricane intensity/track
  - ITCZ
  - Marine stratus – cumulus transition
  - Overland – convective initiation, forecasting for solar energy
- North Atlantic tradewind regional variability
  - Winter – fronts and storm tracks
  - Summer – easterly waves and cyclones
- Uniquely influenced by Saharan dust and African biomass burning
- Rich ocean eddy activity, riverine barrier layers

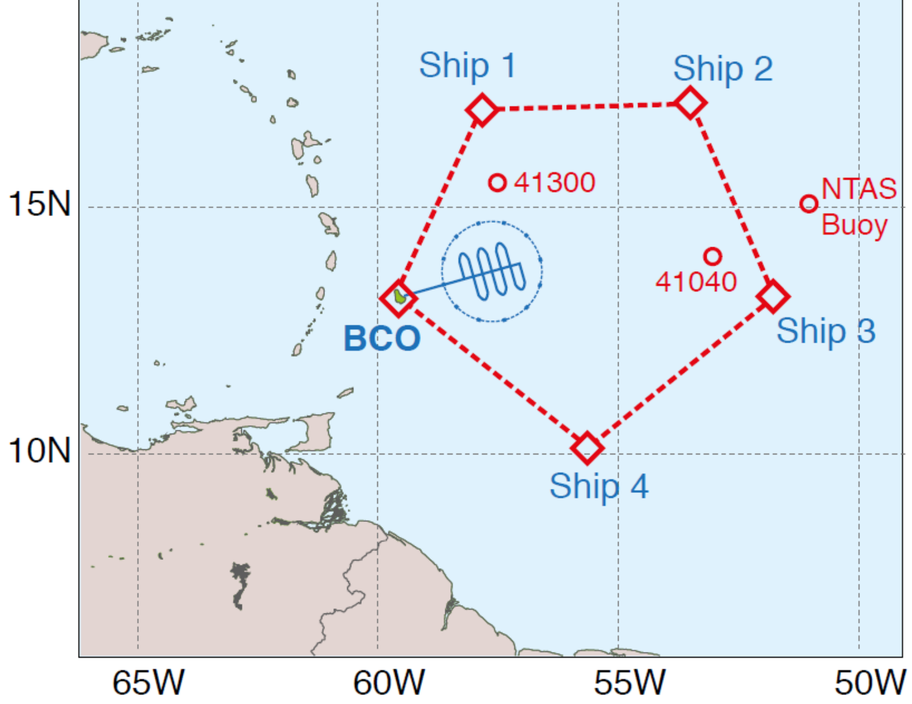
Ship 1
Ship 2
41300
NTAS
Buoy
15N
41040
BCO
Ship 3
10N
Ship 4
65W
60W
55W
50W

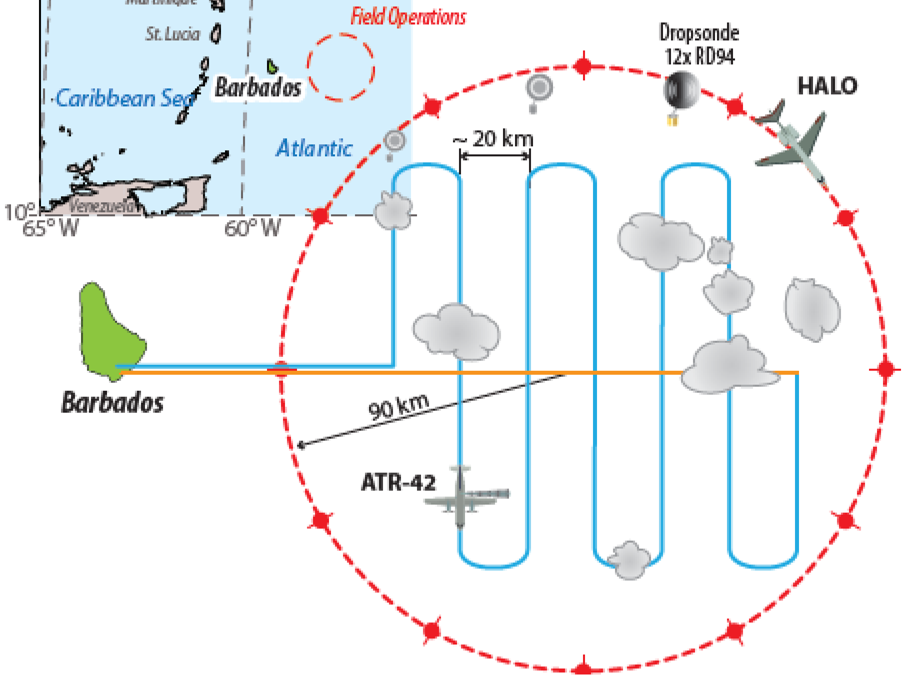
St. Lucia
Field Operations
Dropsonde
12x RD94
HALO
Caribbean Sea
Barbados
Atlantic
~ 20 km
10°
65° W
60° W
Venezuela
Barbados
90 km
ATR-42

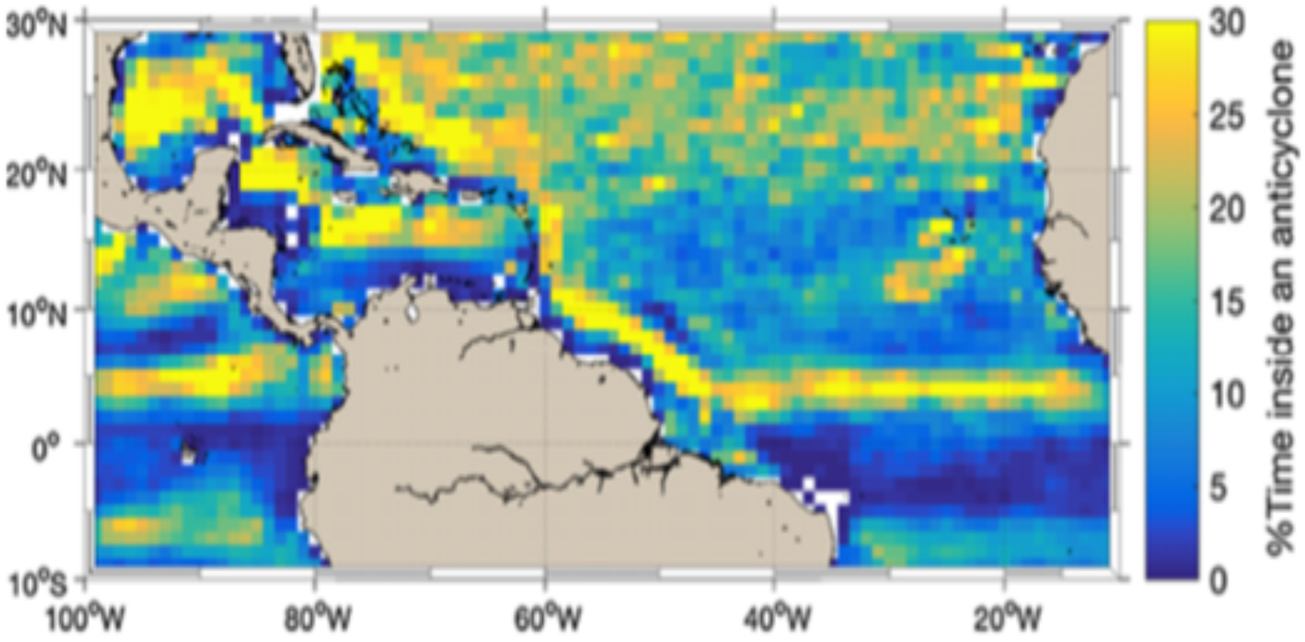
30°N
20°N
10°N
0°
10°S
100°W
80°W
60°W
40°W
20°W
30
25
20
15
10
5
0
% Time inside an anticyclone

NOAA Effort

- NOAA observational assets
  - Ship
  - Aircraft
  - Island-based systems
- NOAA/OAR modeling research
  - Stratocumulus - Shallow convection
  - Data assimilation
  - Stochastic parameterization
  - Air-sea interaction
- NOAA/EMC
  - Collaborate on advances in operational models

recall: no cruises in S. Atlantic contribute to PSD flux database

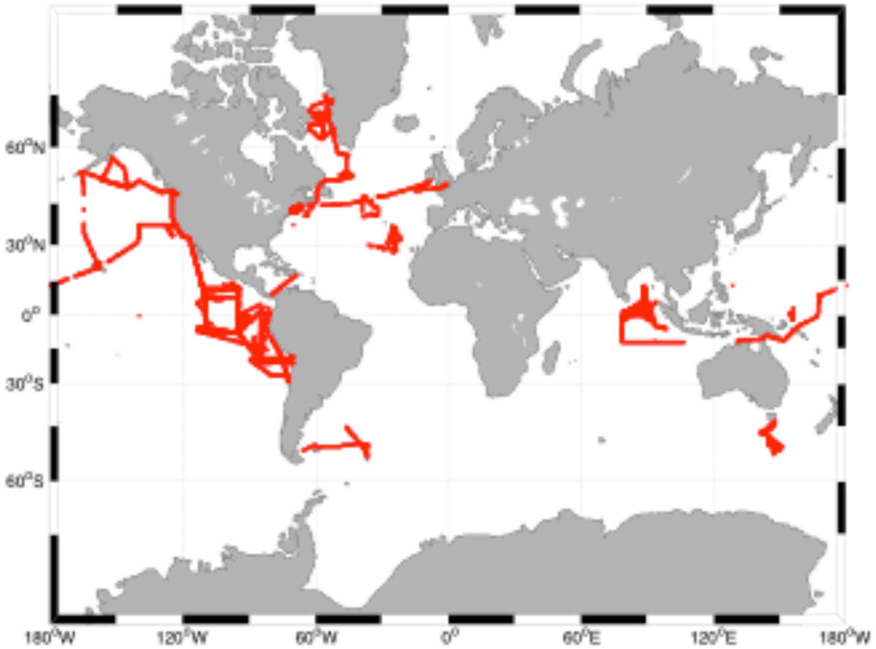

STD Qnet
of 11 products

Products: OAFlux, NOC2, ERAinterim, MERRA, CFSR, ERA40, NCEP1, NCEP2, CORE2, ISCCP, NASA/SRB, CERES

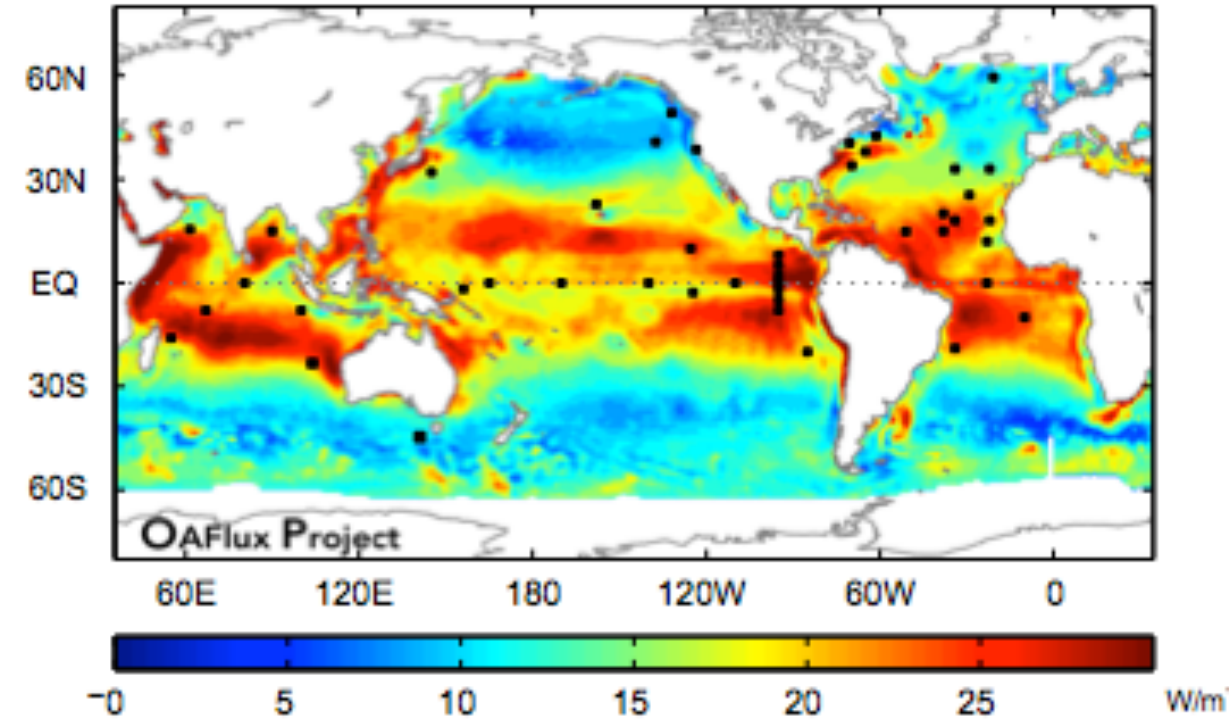

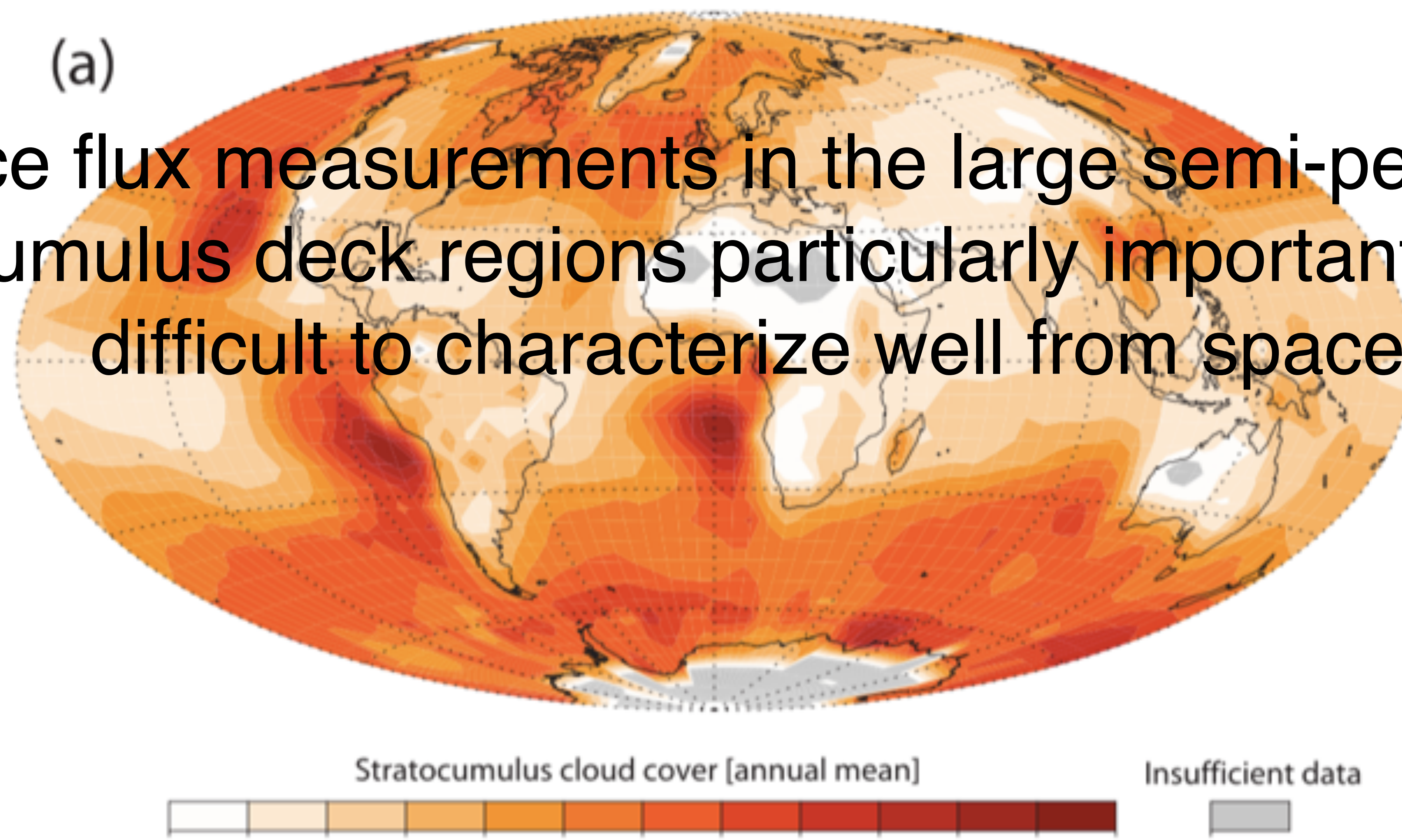

surface flux measurements in the large semi-permanent stratocumulus deck regions particularly important; they are difficult to characterize well from space

Wood 2012

nature geoscience

PROGRESS ARTICLE

PUBLISHED ONLINE: 23 SEPTEMBER 2012 | DOI: 10.1038/NGEO1580

An update on Earth's energy balance in light of the latest global observations

Graeme L. Stephens[1]*, Juilin Li[1], Martin Wild[2], Carol Anne Clayson[3], Norman Loeb[4], Seiji Kato[4], Tristan L'Ecuyer[5], Paul W. Stackhouse Jr[4], Matthew Lebsock[1] and Timothy Andrews[6]

Climate change is governed by changes to the global energy balance. At the top of the atmosphere, this balance is monitored globally by satellite sensors that provide measurements of energy flowing to and from Earth. By contrast, observations at the surface are limited mostly to land areas. As a result, the global balance of energy fluxes within the atmosphere or at Earth's surface cannot be derived directly from measured fluxes, and is therefore uncertain. This lack of precise knowledge of surface energy fluxes profoundly affects our ability to understand how Earth's climate responds to increasing concentrations of greenhouse gases. In light of compilations of up-to-date surface and satellite data, the surface energy balance needs to be revised. Specifically, the longwave radiation received at the surface is estimated to be significantly larger, by between 10 and 17 Wm^{-2}, than earlier model-based estimates. Moreover, the latest satellite observations of global precipitation indicate that more precipitation is generated than previously thought. This additional precipitation is sustained by more energy leaving the surface by evaporation — that is, in the form of latent heat flux — and thereby offsets much of the increase in longwave flux to the surface.

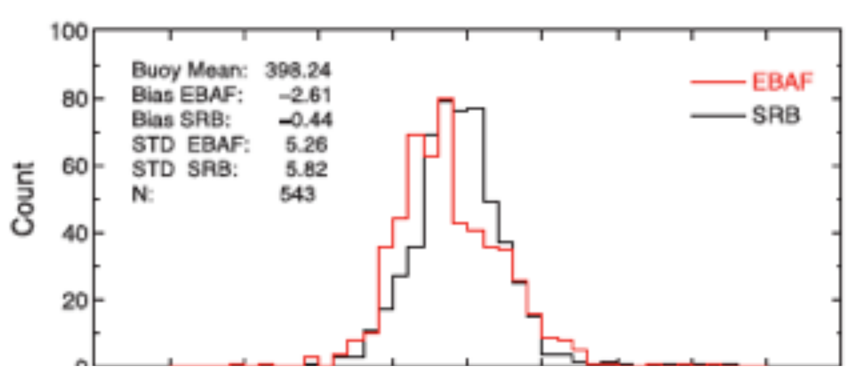

FIG. 7. Histogram of monthly mean downward (top) longwave and (bottom) shortwave irradiance difference; 24 buoy observations from 2001 through 2007 are used. The red line is for EBAF-surface and black line is for SRB surface irradiance (Stackhouse et al. 2011). Numbers shown in the figure are in W m^{-2} except for *N*, which is the number of monthly observations. Note that biases are different from Table 3 because of different number of samples due to matching EBAF-surface, SRB, and surface observations.

the validation of oceanic CERES downwelling infrared surface fluxes based on only 24 buoys worldwide

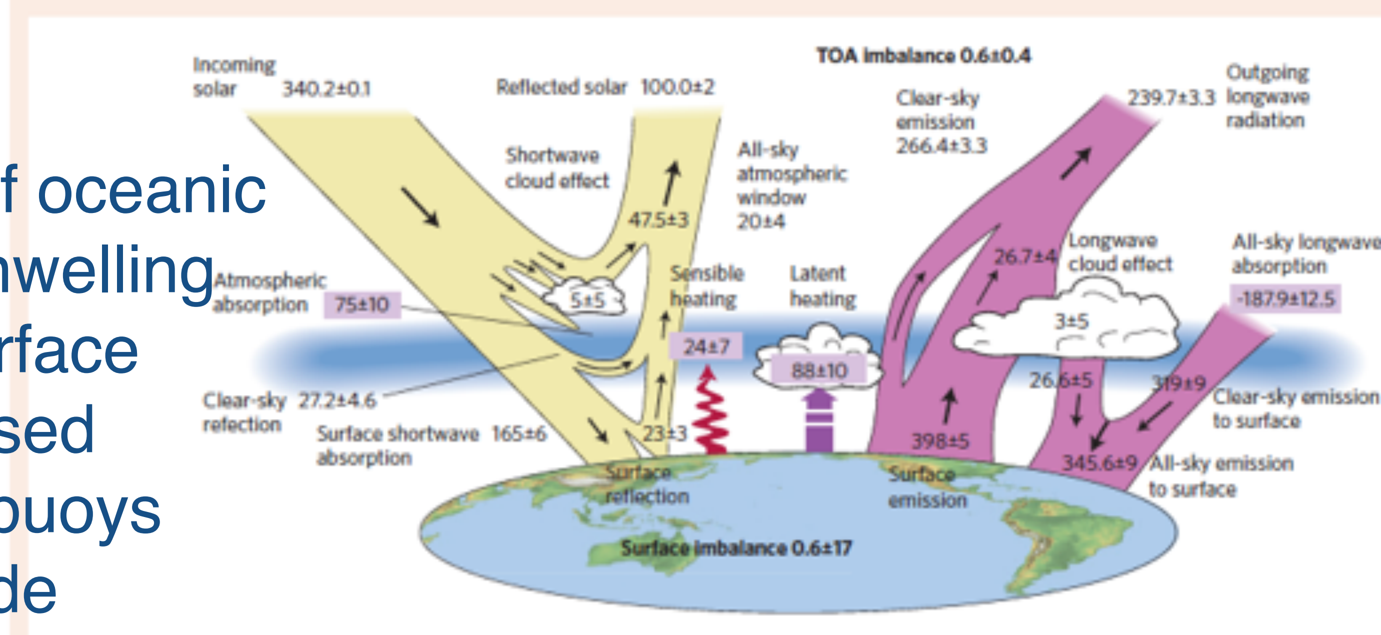

Figure B1 | The global annual mean energy budget of Earth for the approximate period 2000–2010. All fluxes are in Wm^{-2}. Solar fluxes and infrared fluxes in pink. The four flux quantities in purple-shaded boxes represent the principal components of the atmospheric ener

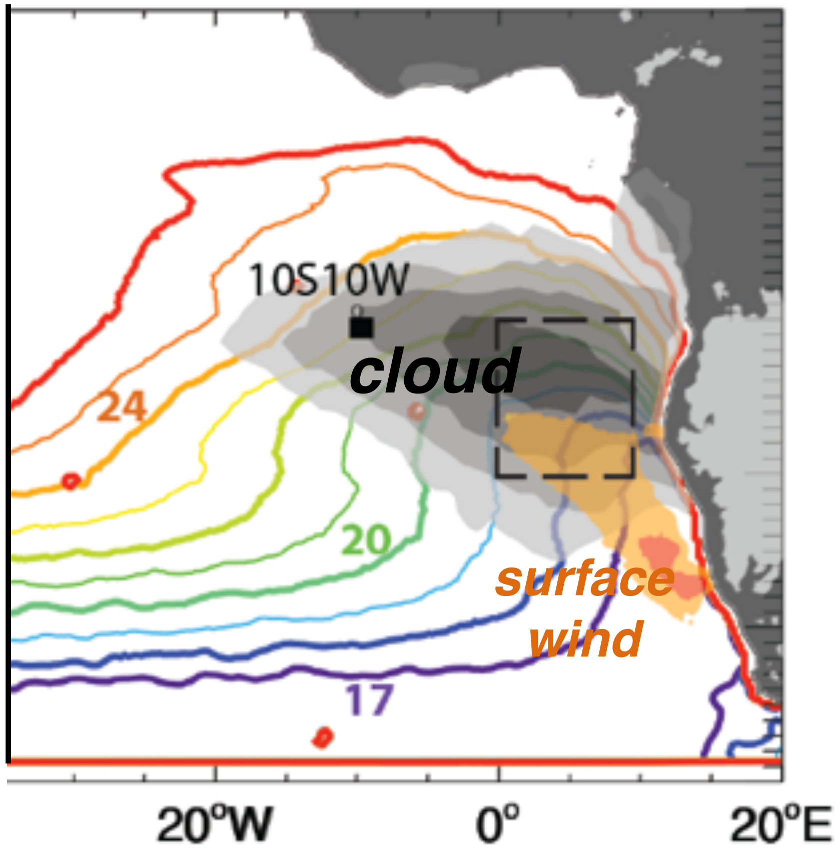

- measurements of the surface fluxes particularly valuable where (low) clouds dominate
- only 2 'full-flux' buoys in the S. Atlantic - 10S,10W and the new PIRATA extension buoy
- bias between buoy-reanalysis products is **not** consistent in sign

Table 1. Annual-mean surface fluxes (W m^{-2}) from buoy, CERES, OAFlux , TropFlux, and ERA-I datasets. Net CERES fluxes in parentheses are calculated using the OAFlux turbulent fluxes. All values are positive downward. The buoy turbulent fluxes are calculated using the COARE 3.0 bulk formulas, with an estimated error of 5 W m^{-2} (Colbo and Weller 2009; Edson et al. 1998). These algorithms are also used in OAFlux and TropFlux. The Stratus buoy sensors were evaluated and calibrated annually for 9 yr (Colbo and Weller 2007; Holte et al. 2014).

	Stratus (20°S, 85°W)[1]						PIRATA (10°S, 10°W)[2]					
	Net SW	Net LW	Net SW + LW	SH + LH	SH	Net	Net SW	Net LW	Net SW + LW	SH + LH	SH	Net
Buoy	191.0	−42.6	148.4	−111.9	−7.4	36.5	219.8	−48.7	171.1	−150.5	−5.4	20.6
CERES	201.1	−39.4	161.7	—	—	(52.4)	224.7	−49.5	175.2	—	—	(38.0)
OAFlux	195.3	−30.0	165.3	−109.3	—	56	223.0	−42.3	180.7	−137.2	−9.9	43.5
TropFlux	175.8	−42.7	133.1	−121.2	−16.8	11.9	209.5	−46.4	163.1	−143.3	−12.0	19.9
ERA-I	207.0	−47.0	160.0	−137.8	−15.4	21.8	229.1	−51.0	178.1	−170.7	−15.0	7.7

[1] 1 Jan 2001–31 Dec 2009.
[2] 1 Jan 2009–31 Dec 2009.

BAMS, 2016, doi:10.1175/BAMS-D-15-00274.1

surface fluxes important for low cloud processes

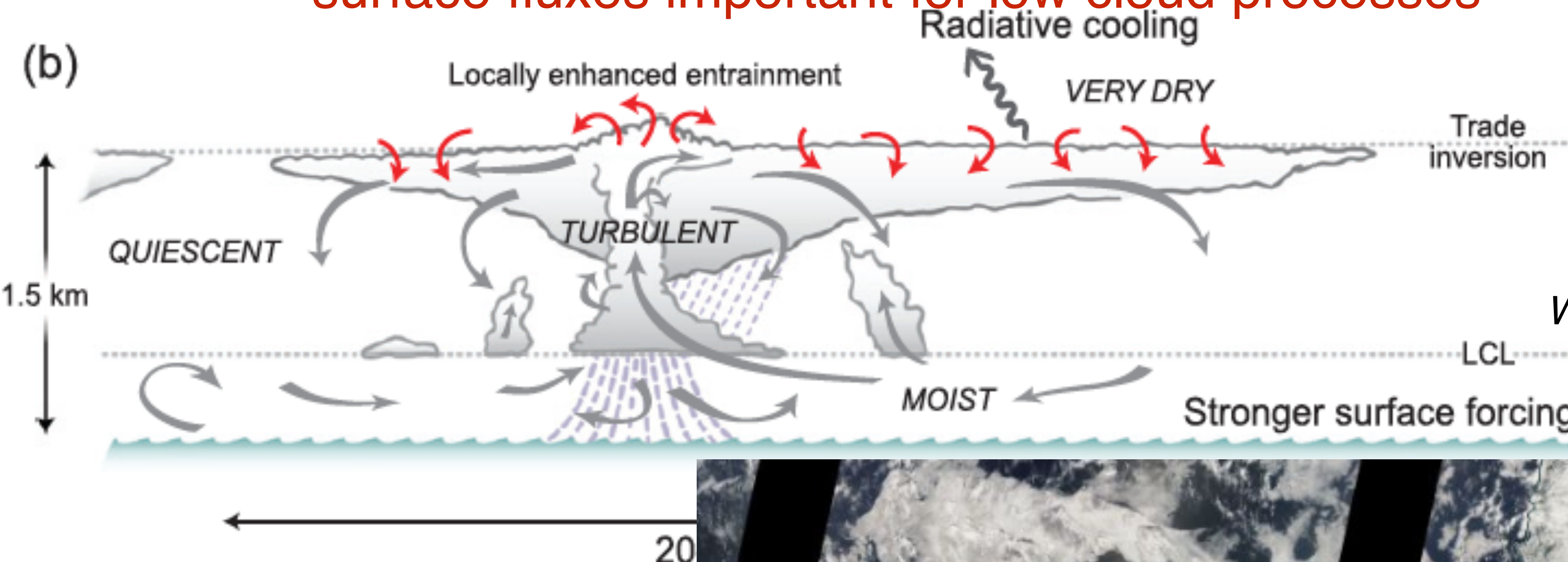

Wood 2012

and for understanding transition from high cloud fraction (stratocumulus) to low cloud fraction (cumulus) conditions

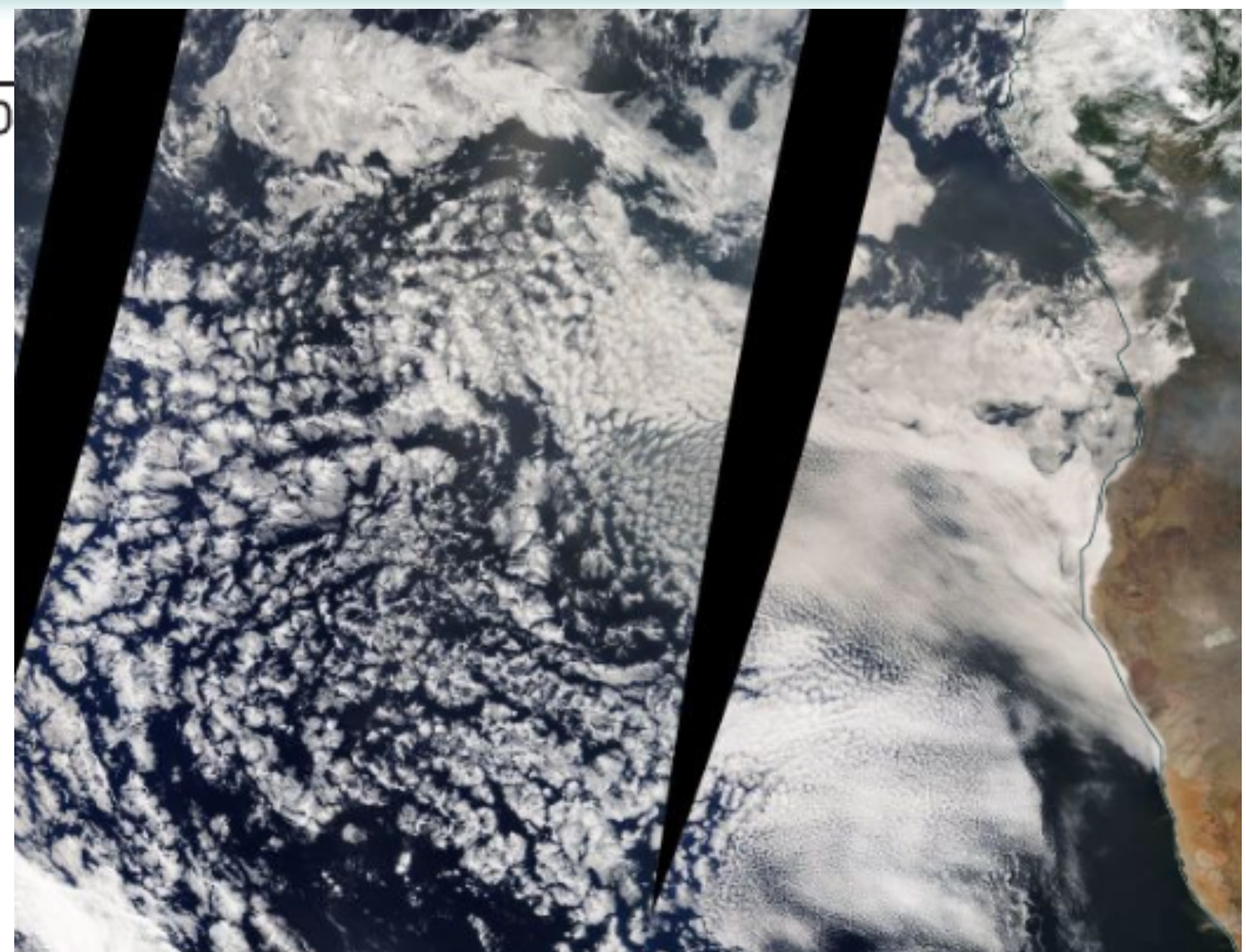

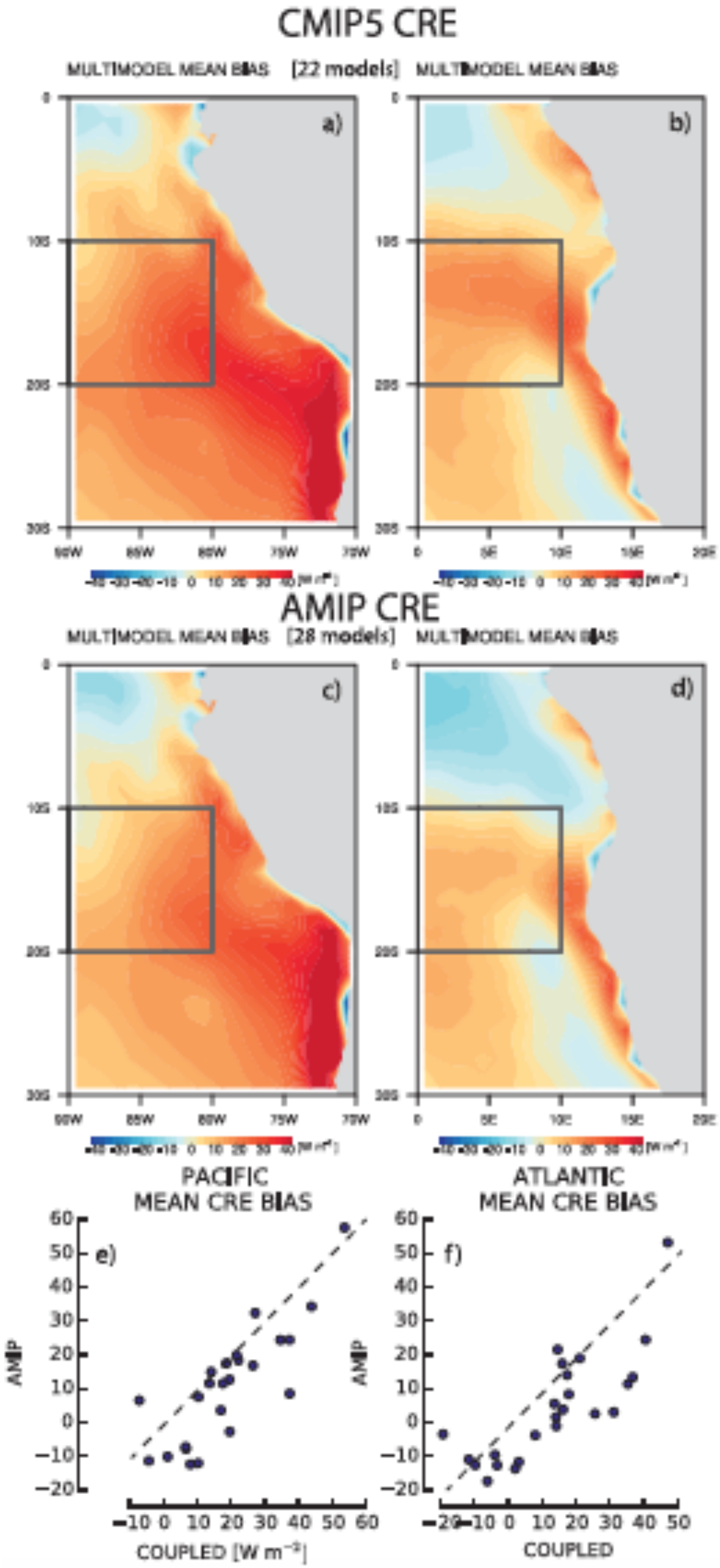

low clouds in turn feedback onto SST

in climate models, composite annual-mean cloud radiative effect (CRE) biases are similar in magnitude in fixed-SST (AMIP) simulations as in CMIP - implicating the atmospheric model component

fig. by Brian Medeiros

BAMS, 2016, doi:10.1175/BAMS-D-15-00274.1

diurnally-resolved observations of SST & PBL profile valuable for evaluating/improving low cloud process studies & model parameterizations

no dedicated effort yet in the southern Atlantic

in contrast to the SE Pacific

Atmos. Chem. Phys., 15, 153–172, 2015
www.atmos-chem-phys.net/15/153/2015/
doi:10.5194/acp-15-153-2015

Atmospheric Chemistry and Physics
Open Access

Global and regional modeling of clouds and aerosols in the marine boundary layer during VOCALS: the VOCA intercomparison

M. C. Wyant[1], C. S. Bretherton[1], R. Wood[1], G. R. Carmichael[2], A. Clarke[3], J. Fast[4], R. George[1], W. I. Gustafson Jr.[4], C. Hannay[5], A. Lauer[6,*], Y. Lin[7,**], J.-J. Morcrette[8], J. Mulcahy[9], P. E. Saide[2], S. N. Spak[2], and Q. Yang[4]

new atmospheric field campaigns focusing on aerosol-cloud interactions: an opportunity (not focused on SST bias improvement per se)

Smoke and Clouds above the Southeast Atlantic

Upcoming Field Campaigns Probe Absorbing Aerosol's Impact on Climate

BAMS, 2016,doi:0.1175/BAMS-D-15-00082.1

focus on August-October months, when 600-700 hPa winds advect biomass-burning aerosol off of continental Africa

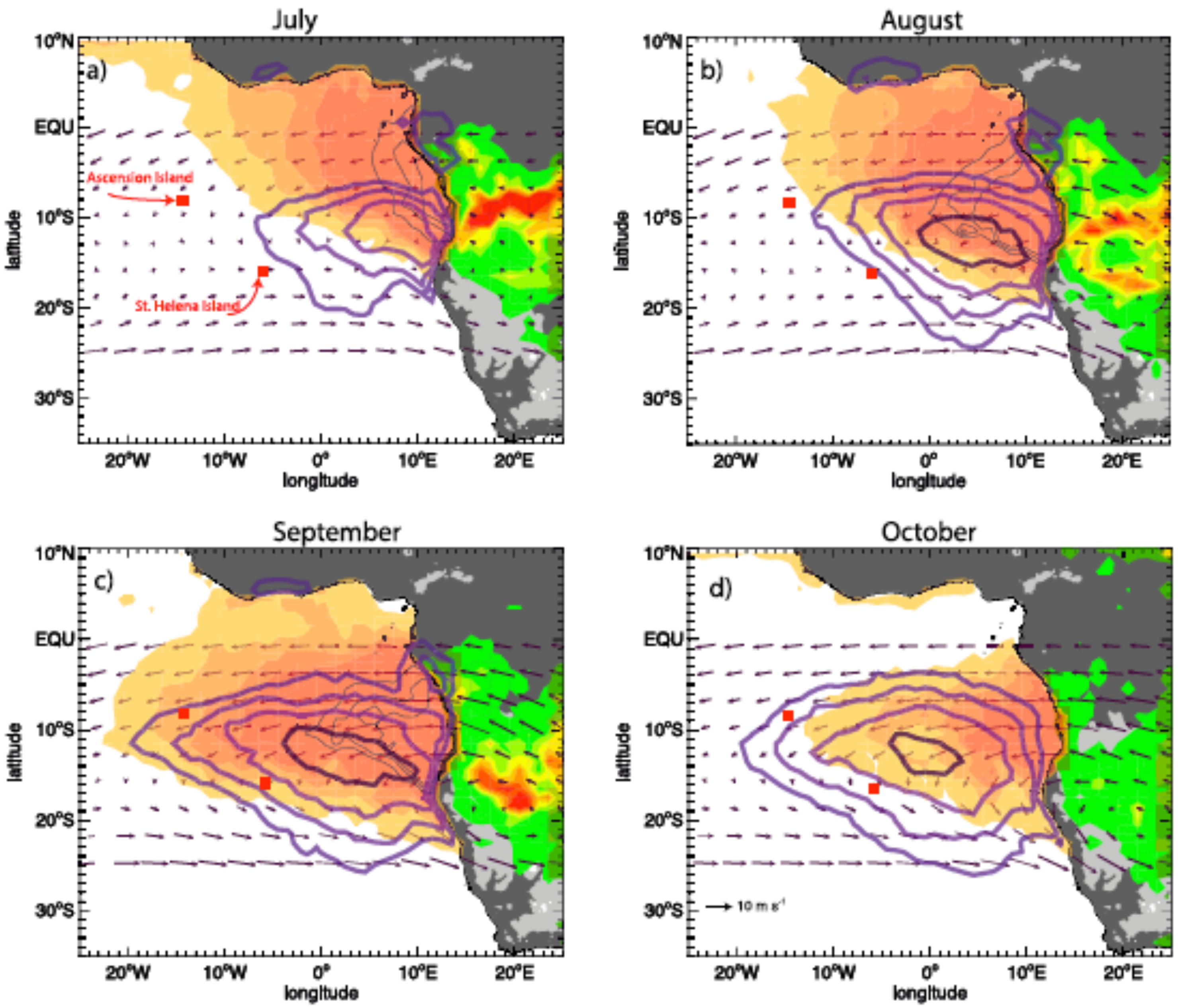

FIG. 5. (a) July, (b) August, (c) September, and (d) October MODIS mean 2002–12 cloud fraction (blue to black contours, 0.6–1.0 increments of 0.1), fine-mode aerosol optical depth (yellow-red shading indicates 0.25–0.45 in increments of 0.05 and very light black contour lines indicate 0.5–0.7 in increments of 0.1), fire pixel counts (green–red shading, 10–510 in increments of 50), and ERA-Interim 2002–12 monthly-mean 600-hPa winds. Red squares indicate Ascension Island and St. Helena Island.

NASA ORACLES flight coverage

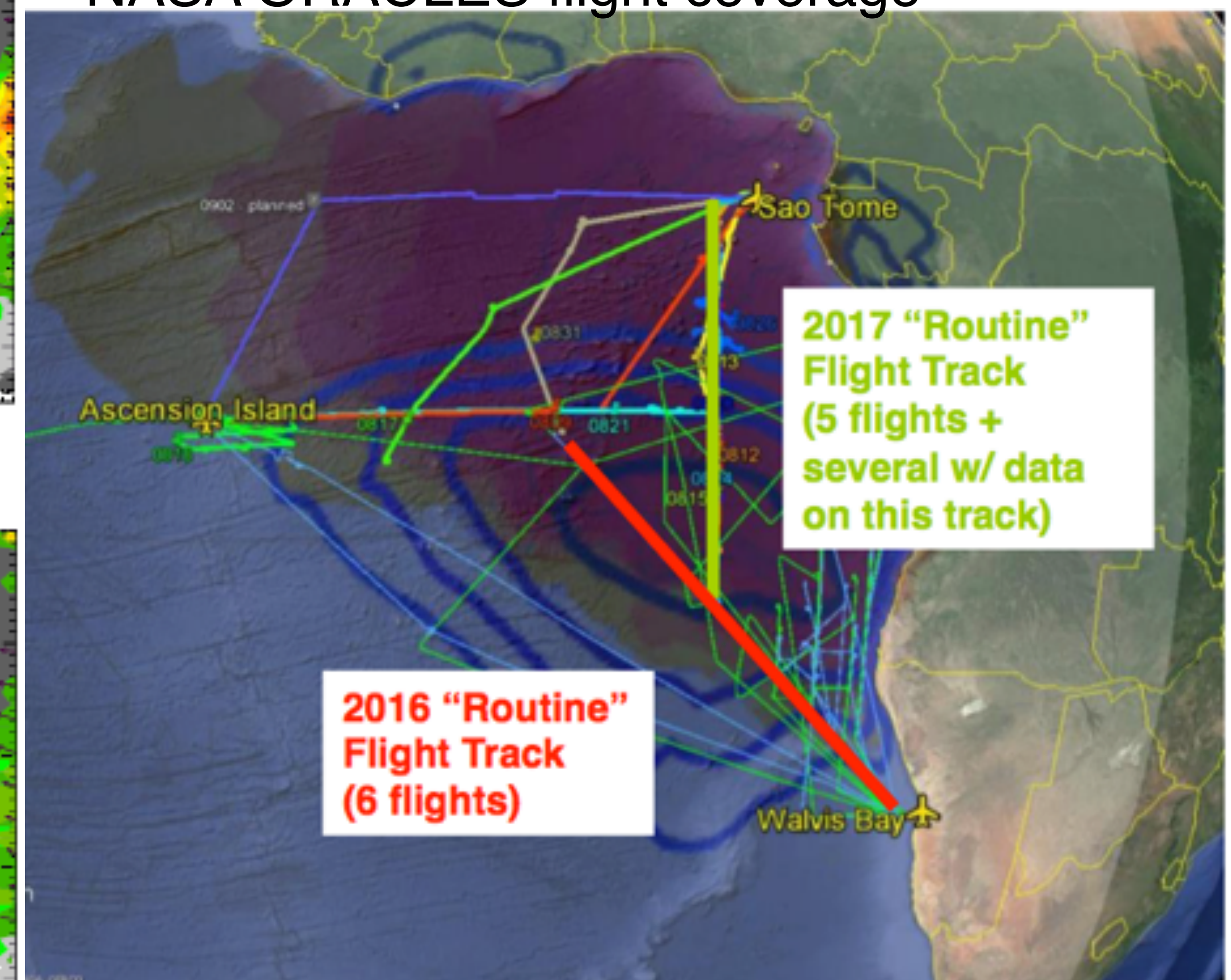

Adebiyi et al , JCLI, 2015

US DOE Mobile Facility deployment to Ascension Island, June 1, 2016 - October 31, 2017

Ascension in trade-wind shallow Cu region

4 to 8x/daily radiosondes is unprecedented in Atlantic

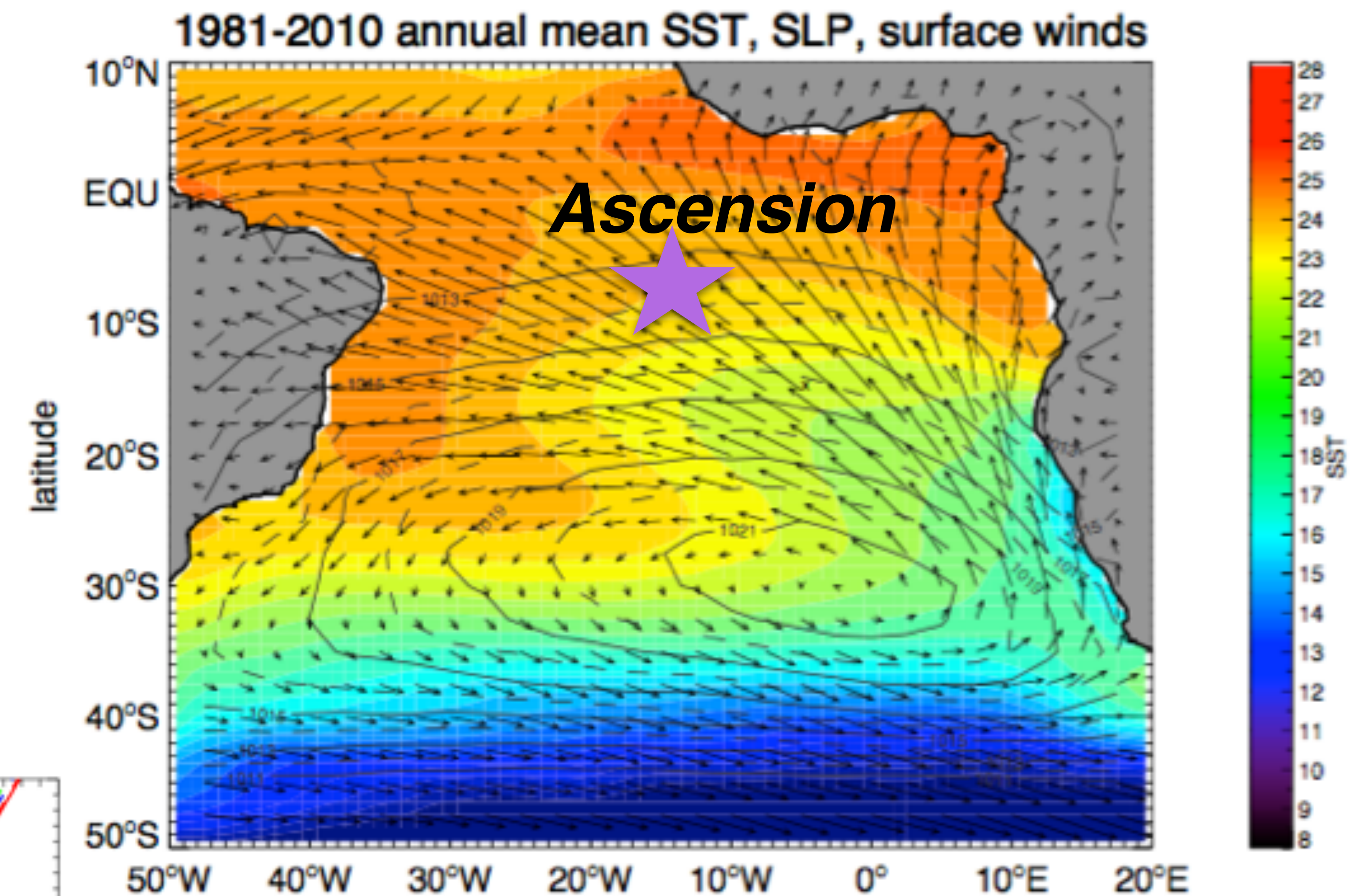

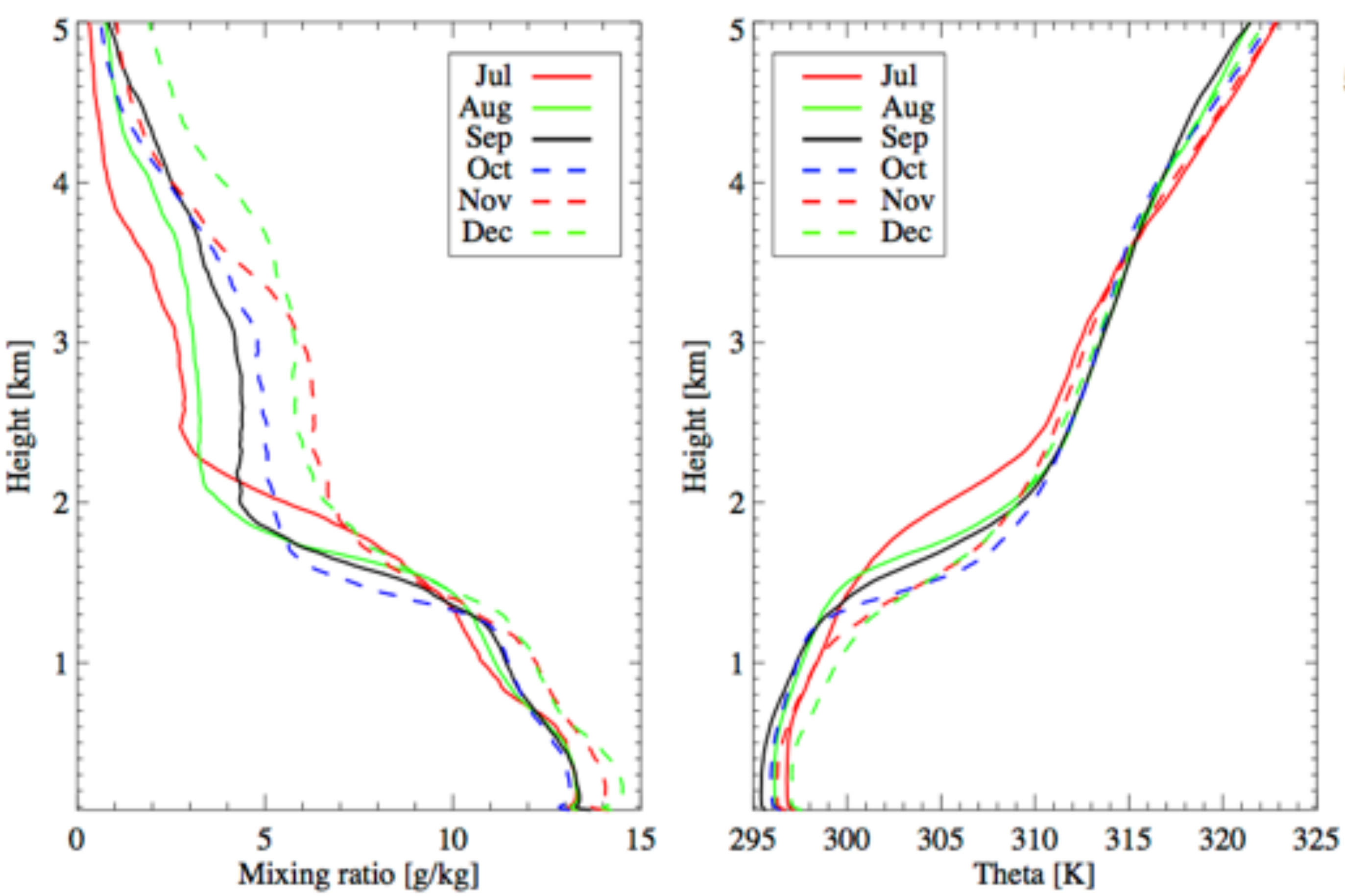

8S, 14W ~9 km to a side

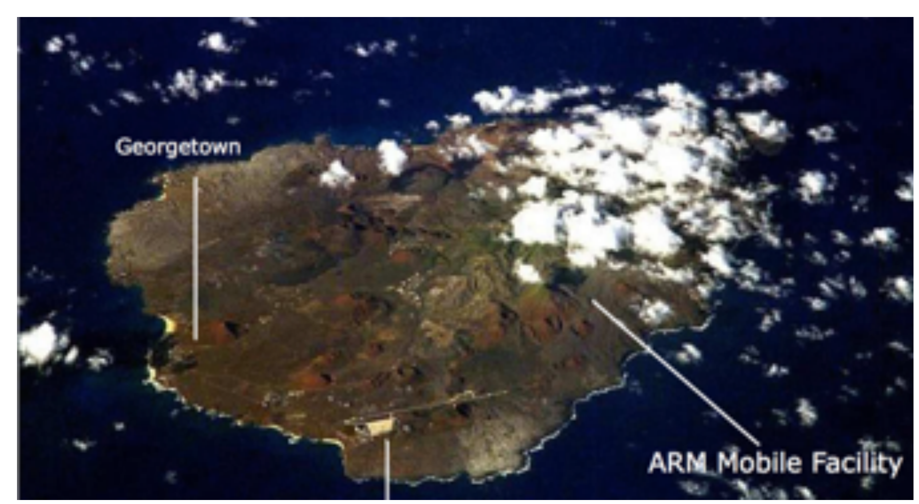

Ascension also a TCCON site (column CO2)

the connection to models

AEROCOM is a community initiative to compare across global aerosol (climate) models. One project highlighted that

- the absorbing aerosols provide a climate warming over the southeast Atlantic
- but individual model direct aerosol radiative effect estimates differ in sign
- cause may be the underlying cloud fraction

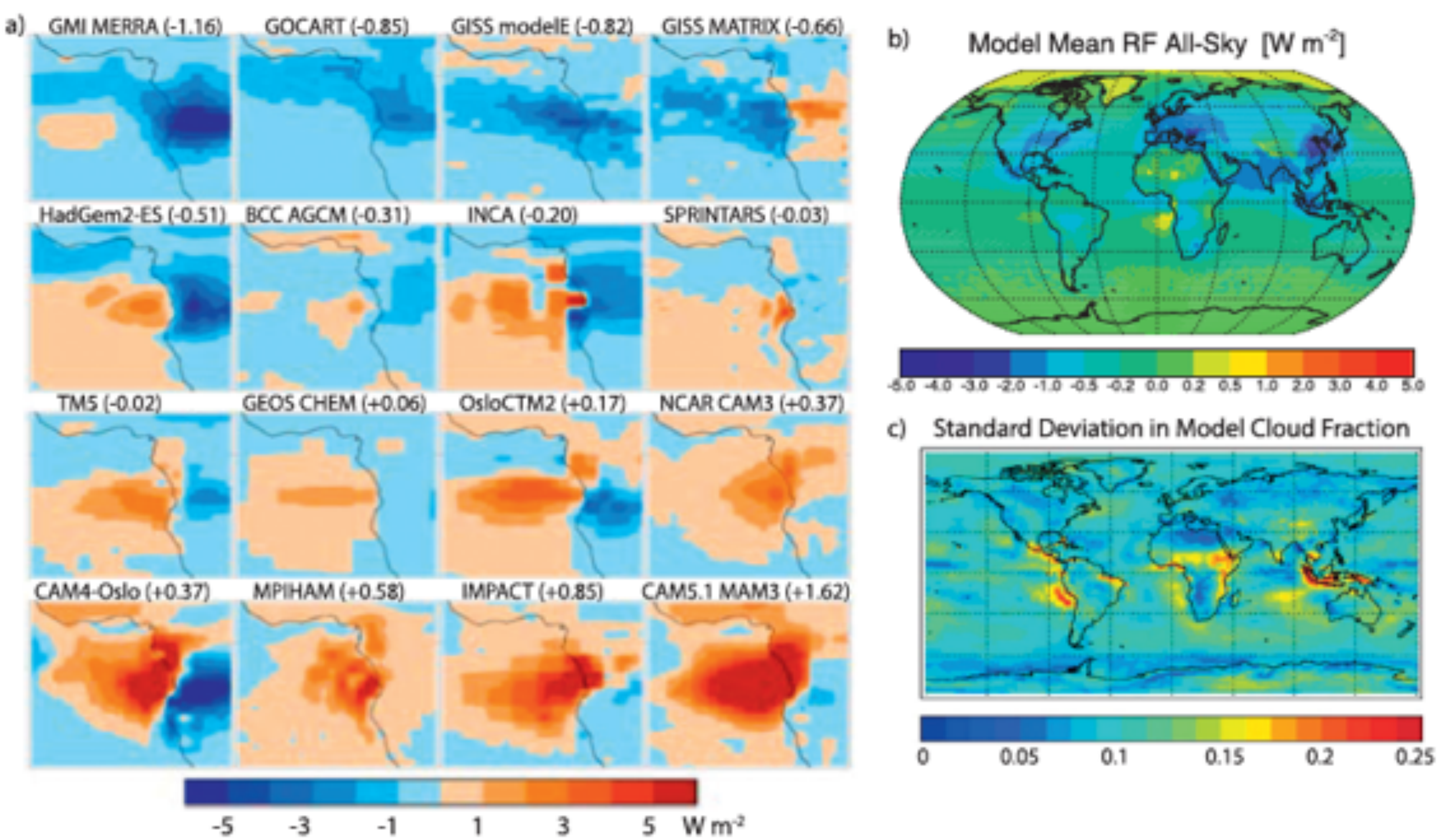

Fig. 2. Modeled Aug–Sep direct aerosol radiative forcing in (a) individual AeroCom models ordered by their regional- and annual-average difference from the (b) ensemble mean indicating the regional hotspot for BB aerosol forcing over the southeast Atlantic. (c) indicates the large diversity in the models' cloud fraction. The cloud fraction helps determine if the aerosol shortwave absorption influences the climate more than the aerosol scattering. More model details can be found in Stier et al. (2013).

campaigns working together
to develop a framework
for model/obs comparison
(through data aggregation)

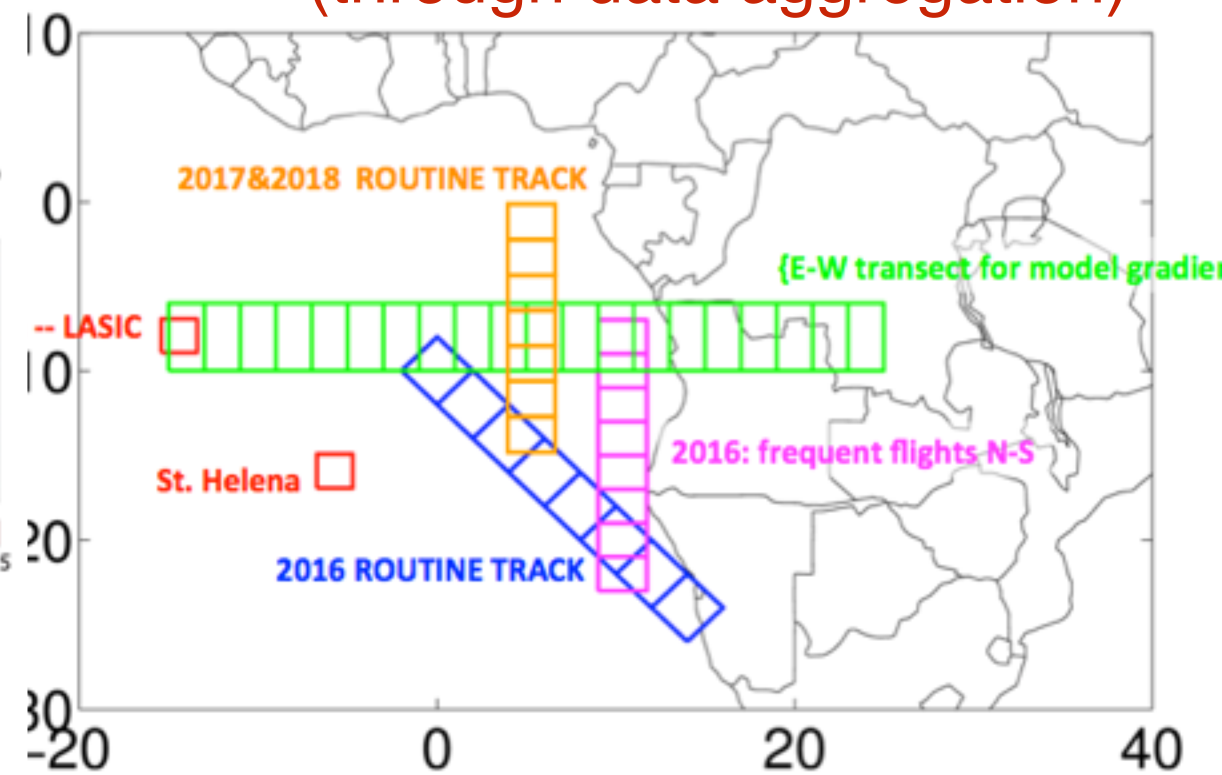

BAMS, 2016,doi:0.1175/BAMS-D-15-00082.1

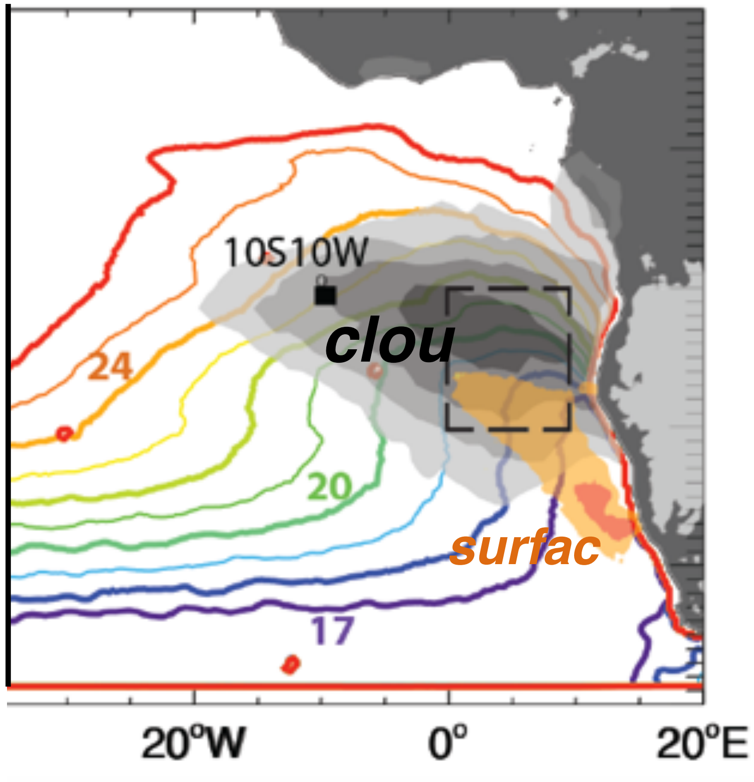

- SST biases largest in the oceanic upwelling regions
- these will affect low cloud cover biases downstream
- Atlantic SST biases related to depiction of low-level winds

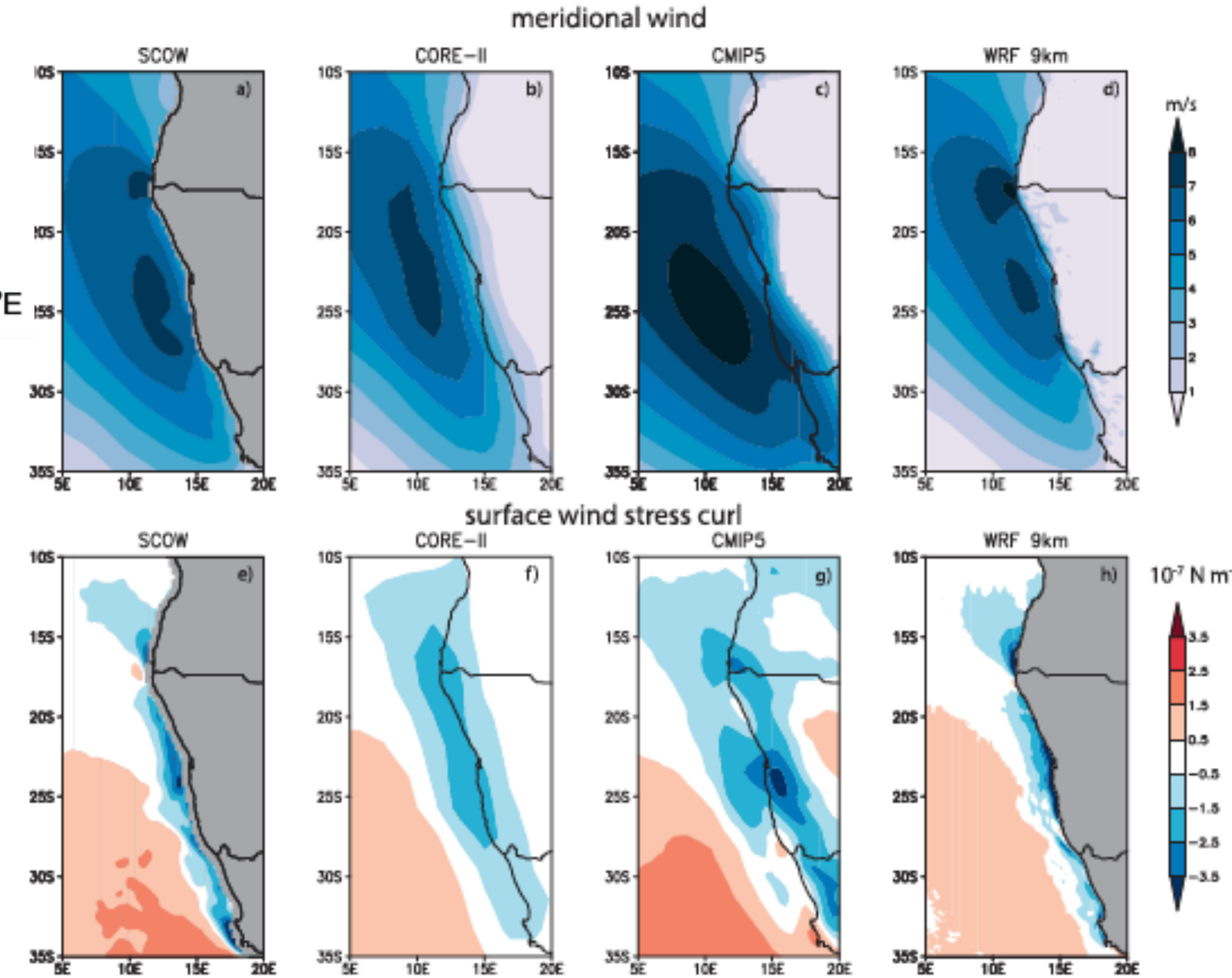

Fig. 12. Coastal southeast Atlantic (a)–(d) meridional winds at 10 m and (e)–(h) surface wind stress curls differ significantly between observations and models and depend on spatial resolution: (a),(e) 0.25° SCOW ocean surface wind vectors, averaged 1999–2009; (b),(f) 1° CORE2 ocean forcing dataset, averaged 1999–2009; (c),(g) CMIP5 multi-model mean, averaged 1984–2004; and (d),(h) a 9-km simulation with the Weather Research and Forecasting Mode averaged 2005–08. See further discussion in Patricola and Chang (2016, manuscript submitted to *Climate Dyn.*)

Patricola and Chang, 2017, Climate Dynamics

Summary, Needs

- diurnally-resolved measurements of the atmospheric boundary layer are lacking (except now at Ascension); useful for low cloud process studies (stratocumulus to cumulus transition) and parameterization development

- need more full-flux (downwelling infrared) buoy measurements, also for space-based remote sensing

- need more atmospheric boundary layer measurements in upwelling regions